ERASMUS +: ERASMUS MUNDUS MOBILITY PROGRAMME

Master of Science in

COASTAL AND MARINE ENGINEERING AND MANAGEMENT

CoMEM

STABILITY OF BLOCK MATTRESSES UNDER NON-UNIFORM FLOW

Delft University of Technology
3th July 2017

Xabier Arrieta

The Erasmus+: Erasmus Mundus MSc in Coastal and Marine Engineering and Management is an integrated programme including mobility organized by five European partner institutions, coordinated by Norwegian University of Science and Technology (NTNU).

The joint study programme of 120 ECTS credits (two years full-time) has been obtained at two or three of the five CoMEM partner institutions:

- Norges Teknisk- Naturvitenskapelige Universitet (NTNU) Trondheim, Norway
- Technische Universiteit (TU) Delft, The Netherlands
- Universitat Politècnica de Catalunya (UPC). BarcelonaTech. Barcelona, Spain
- University of Southampton, Southampton, Great Britain
- City, University London, London, Great Britain

During the first three semesters of the programme, students study at two or three different universities depending on their track of study. In the fourth and final semester an MSc project and thesis has to be completed. The two-year CoMEM programme leads to a multiple set of officially recognized MSc diploma certificates. These will be issued by the universities that have been attended by the student. The transcripts issued with the MSc Diploma Certificate of each university include grades/marks and credits for each subject.

Information regarding the CoMEM programme can be obtained from the programme coordinator:

Øivind A. Arntsen, Dr.ing.
Associate professor in Marine Civil Engineering
Department of Civil and Transport Engineering
NTNU Norway

Telephone: +4773594625 Cell: +4792650455 Fax: + 4773597021

Email: oivind.arntsen@ntnu.no

CoMEM URL: https://www.ntnu.edu/studies/mscomem

CoMEM Master Thesis

This master thesis was completed by:

Xabier Arrita
Email: arrieta.xabi@gmail.com

As a requirement to attend the degree of:

Erasmus+: Erasmus Mundus Master in Coastal and Marine Engineering and Management (CoMEM)

Under the supervision of:

Prof.dr.ir. Uijttewaal, W.S.J.	*TU Delft*
Ir. Verhagen	*TU Delft*
Ing. Kuiper, C.	*TU Delft*
Mr. Quataert	*Holcim Coastal B.V.*

In collaboration with:

Delft University of Technology
Faculty of Civil Engineering and Geosciences
Department of Hydraulic engineering

Holcim Coastal B.V.

This master degree was taught at the following educational institutions:

- Norges Teknisk- Naturvitenskapelige Universitet (NTNU) – Trondheim, Norway
- Technische Universiteit (TU) Delft – Delft, The Netherlands
- University of Southampton - Southampton, Great Britain

At which the student has studied from August 2015 to July 2017.

Preface

This thesis was developed as the graduation process of Master of Science in Coastal and Marine Engineering and Management (CoMEM). The work has been carried out at for the Hydraulic Engineering Section of the Delft University of Technology and together with the support of Holcim Nederland B.V. The experiments were conducted in the Fluid Mechanics Laboratory under the supervision of Sander De Vree.

This thesis can be seen as an extension of the previous findings by Smyrnis (2017), also developed under the support of Holcim Nederland B.V. The tested block mattress, Betomat is a registered trademark of Holcim betonprodukten bv, Aalst, Netherlands.

I would like to thank to my committee, Mr. Verhagen, Prof. Uijjtewaal and Mr. Kuiper for all the support during the thesis.

I would like to thank to Mr. Quataert and Mr. Albrechts on behalf of Holcim Coastal B.V. for their essential support on the development of this thesis.

I would also like to thank to all the staff of the laboratory for their assistance during the experiments.

Finally, I would like to mention that it was a pleasure to develop this thesis in parallel with Teri Tian and that the team we built up was indispensable, especially during the experimental process.

Abstract

Block mattresses are widely used bed protection elements under non-uniform flows. Previous studies show that the turbulence of the flow plays a key role on the instability of the mattress. However, in the available design equations, the turbulence intensity is included as a magnification factor roughly and qualitatively defined. Consequently, the design equations are often used as a rule of thumb, where the engineering criteria of the designer is critical and large safety factor are used.

Therefore, the development of a design equation for non-uniform flow is needed. Besides, the understanding of the failure mechanism of the block mattress and the influence of the turbulent fluctuations on stability should be studied. For this purpose, and extended literature review and a series of tests were done measuring the flow downstream a weir, to analyse the failure mechanism and derive an innovative design equation developed under non-uniform flow.

In turbulent non-uniform flows, the available design equations were developed for uniforms flow and the turbulent intensity is included as a magnification factor, usually poorly defined. The stability reduction due to turbulence has been proved by several authors. However, there is not any study in previous literature that investigate the role of velocity fluctuations on block mattress failure.

Nevertheless, the literature review showed that an innovative approach, which combines the mean velocity and the turbulence intensity to quantify the flow forces, has been largely study for loose rock by several authors. Following this trend, the option of applying this structure $\left(\bar{u} + \alpha\sqrt{k}\right)$ as a flow quantification on Pilarczyk equation was decided to study.

For this purpose, a series of test were done under four different configurations. Two weir heights were used (15 and 18.5cm) and the distances corresponding to 3h and 4h were checked. Four failures were recorded for each configuration for a total of 16 failures. Additionally, a data base was recorded for each configuration where the flow discharge was related to mean velocity and the turbulence intensity.

An analysis of the failure mechanism was done by synchronizing the velocity time series with the displacement of the blocks. The results showed that an episode of peak streamwise velocity and downwards (sweep) was present at the failure. However, the analysis of the velocity showed that higher combinations of streamwise velocity and shear stress were present before the failure on almost all the records.

Therefore, the streamwise velocity and the induced shear stress cannot solely explain the failure of the block mattress. This conclusion is in line with the work done by Hofland (2005). However, the recorded data did not allow to describe completely the failure mechanism. In section 6.4, the possible explanations were discussed and the recommendations for further researches were described.

Moreover, the failure of the block mattress was located at the last row of the block mattress. The flow around the last block was studied and the behaviour of the flow over an open edge and a close edge was compared. The tests showed that the last block acts as a backwards facing step accelerating the flow with Froude numbers close to 1. Additionally, the presence of adjacent blocks on middle blocks and close edge provides extra cohesion between the block, increasing the stability.

The turbulence magnification factor (α) at the stability equation was derived by two different approaches. The first approach was based on the peaks of velocity associated to failure while the second one was described as a fitting parameter. The analysis concluded that the α values were close to 3 for both cases, in line with the expected value from previous studies. Besides, the stability parameter was derived. The comparison between approaches concluded that the first approach was more conservation while the second one provides more accurate values. In addition, the developed data base shows that the flow parameter as mean velocity and turbulence intensity can be related to the weir structure, the apron length and the flow discharge.

Finally, the new developed equation was compared with the original Pilarczyk equation and the modification proposed by the Rock Manual (2007). The comparison shows that the new developed equation described the required thickness of the block more accurately than the available equations. Thus, the results show that the proposed approach described the effect of turbulence accurately on a design equation. Additionally, all the relevant derived conclusions for design propose were summarized in a design guideline.

Contents

1. Introduction

Scour protection is nowadays one of the most relevant topics at hydraulic engineer. The presence of a hydraulic structure leads to perturbations of the flow that usually induce scour of the bed. The scour holes that can threaten the stability of the structure and become a main failure cause (Kang et al., 2011). Block mattresses are common protection elements used to reduce the erosion downstream of structures, due to economics, lack of suitable stone, ease of placement and visual appearance (Escarameia and May, 1992).

1.1 Problem definition

Block mattresses are commonly placed downstream of different hydraulic structures like sluice gates, culverts, weirs or spillways where turbulence is highly present. Several stability equations are available on literature, but they do not take quantitative account on highly turbulent flows (Escarameia and May 1995). The quantitative approaches to turbulence effect are based on rip rap stability, note Jongeling et al, (2003), Hofland (2005) and Hoan (2008). However, results obtained by Smyrnis (2017) proved that the level of turbulence are more crucial for the stability of block mattresses than the mean flow velocity.

Moreover, the failure of mattresses is sudden and once the mattress has been lifted, the drag forces increase leading to further uplift and total removal (Van Velzen and De Jong 2015). Thus, there is a major necessity of deriving an equation that considers a quantitative account on turbulence regarding the stability of concrete block mattresses.

1.2 Objective

The objective of this M.Sc. thesis can be summarized as the stability of block mattresses under non-uniform flows. For hydraulic engineering, design guidelines (supplied by manufactures) are more used than design codes due to the empirical nature of the present design process (Pilarczyk 2003). Hence, this project will be focus on setting up the base of a design guideline of Betomat block mattresses supplied by Holcim.

The objectives of this thesis can be described in three main research questions: (i) Detailed knowledge of how the combination of mean flow and turbulence fluctuations induce failure of the block mattress. (ii) Derivation of a block mattress stability equations that includes the turbulence intensity in a quantitative way. (iii) The derivation of a relation between the characteristic of the structure and the flow parameters.

1.3 Methodology

The objectives mentioned in section 1.2 are achieved by the following methodology. First, an extensive literature is done. This provides relevant information of block mattresses stability, but also about the stability equations derived for granular bed

protections. The existing equations show that the existing equations for block mattresses do not include accurately the turbulence fluctuations. The lack of available data exposes the need of experimental research to collect data.

The stability of block mattresses downstream of a weir is checked for four different configurations. Based on the collected data on the flume tests, the influence of the turbulence fluctuations on the failure mechanism is studied. Also, a new stability equation is derived based on the obtained data.

Additionally, the new developed equation is compared with the previously existing equations and finally the obtained results are discussed and summarized. Besides, all the relevant information for designing is summarized is a design guideline.

2. Literature review

In this chapter, the background information relevant for the understanding and development of this thesis is presented. As the studies of the stability under non-uniform flow for block mattress are not very present in literature, some other related topics are also presented.

In section 2.1 the turbulent flow characteristics are discussed as well as the effects of weirs in the flow. The block mattress characteristics, the acting forces on them and their failure mechanisms will be studied in section 2.2. In section 2.3, the stability equations for block mattresses and for stones under non-uniform flow will be analysed. The conclusions and the summarizing of relevant remarks is present in section 2.4

2.1 Turbulent flow

Turbulence

Turbulence was defined per Hinze in 1975 (In Schiereck 2012) as: "Turbulent fluid motion is an irregular motion, but statistically distinct average values can be discerned and can be described by laws of probability". Thus, even the chaotic nature of turbulence, it can be expressed as a statistical parameter. The instant velocity can be described as the addition of an average component that is constant over a period and the turbulent fluctuations over the average.

$$u = \bar{u} + u' \qquad v = \bar{v} + v' \qquad w = \bar{w} + w' \qquad [2.1]$$

Those fluctuations are of major importance since the forces generated by turbulence dominate the mean forces ((Einstein 1949) In Hoan 2008). Hence, is necessary to obtain a measurement of the intensity of those velocity fluctuations. The average value of all the fluctuations is zero by definition, so the squares of the fluctuations are used to average. The turbulence intensity is defined as the square root of this average and has the same dimensions as velocity (Schiereck 2012). Thus, the turbulence can be computed as the standard deviation of the velocity fluctuations [2.2]. Moreover, other expressions can be used to characterize turbulence:

$$\sigma_u = \sqrt{\frac{1}{N}\sum_{i=1}^{N}(u_i - \bar{u})^2} \qquad [2.2]$$

$$k = \frac{1}{2}\left(\overline{u'^2} + \overline{v'^2} + \overline{v'^2}\right) \qquad [2.3]$$

$$r_u = \frac{\sqrt{\overline{u'^2}}}{\bar{u}}, r_u = \frac{\sqrt{\overline{v'^2}}}{\bar{v}}, r_w = \frac{\sqrt{\overline{w'^2}}}{\bar{w}} \qquad [2.4]$$

Equation 2.4 provides the total kinetic energy in a turbulent flow, while equation 2.3. computes the relative fluctuation intensity in each of the flow components.

The standard deviation of the velocity components was approximated by Nezu and Nakanawa (in Hofland 2005). Equation 2.5 shows that an increasing turbulence is related to an increasing friction velocity (u_*). Hence, it can be derived that turbulence intensity is directly related to instability and sediment transport.

$$\frac{\sigma(u_i)}{u_*} \approx \alpha_i e^{-y/h} \qquad [2.5]$$

The values given for empirical factor α_i are: $\alpha_x = 2.30$, $\alpha_y = 1.27$, $\alpha_z = 1.67$

Coherent structures

Although turbulent flows are chaotic and highly variable, there are flow patterns and structures that can be observed repeatedly. Hofland (2005) call them 'Coherent structures'. It was concluded that the transport of stones at low patterns is mainly determined by the extreme value of the fluctuating forces. If these extreme forces can be linked to a certain kind of flow structures, then a model for damage of bed protection can be based on characteristics of this structure.

Raupach (1981) (in Thompson 2017) presented a quadrant analysis to point measurements of a rough bed flow. This analysis was based on the pair values of u' and w' and their effect on instantaneous Reynolds's stresses. The combinations of Q2 (u'< 0 and w' > 0) called ejection and Q4 (u'> 0 and w' < 0) called sweep are the most frequently occur combinations and they are straight related to initiation of movement (Thompson 2017)

Turbulence over a weir

The scope of this thesis is limited, as mentioned above, to the turbulence generated downstream of a weir. Weirs are very common hydraulic structures with several fundamental functions like water level management, flow measurement, environmental enhancement or channel stabilization (Ibrahim, 2016).

Downstream of a weir, complex three-dimensional flow phenomena involving significantly curved streamlines and vortex structures can take place (Gharahjeh, Aydin and Altan-Sakarya, 2015) creating a considerable amount of turbulence.

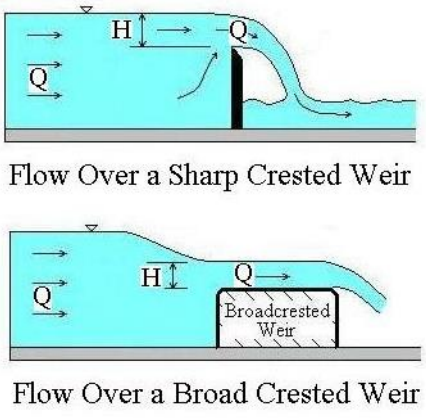

Figure 2.1: Flow over a weir (Brighthub Engineering, 2017)

The influence of the turbulence induced by a weir at the downstream bed material has been previously studied. However, in most of the cases it has been focussed on the scour of bed material (Ibrahim 2015, 2016, Sobeih et al., 2012). Which is a completely different approach from the stability of a block mattress.

In literature, different studies have induced turbulence on the flow by different approaches. In Hoan (2008), for example, by lateral expansions of the channel over a flatbed covered by stones. Smyrnis (2017) proved the qualitative effect of turbulence on the stability by disturbing the flow with the hands. Besides, it is expected that the knowledge and conclusions derived from this study can be useful for a broad range of flow situations.

2.2 Block mattres

During the tests, the stability of the Betomat block mattress supplied by Holcim will be tested. A block mattress is composed by a geotextile and a series of concrete units that provide stability. Holcim provides varied sizes of concrete blocks to withstand the different loads applied. A mattress is form by the combination of sixty blocks placed regularly that leads to maximum dimensions of 2.40 m (width) per 6.00 m (length). Hence, the combination of multiples concrete mattresses is a common practise on bed protection. At the edge of the mattress the geotextile is extended beyond the contour of the block. This extra part of the geotextile is used to lifting and placing the mattress as well as to facilitate a good overlap between mattresses.

Although the present study has been done only for a specific type of block mattress, it is expected that the out coming conclusions and recommendations can be used for the design of different prototypes of concrete block mattresses.

Annex 1 provides more information about the studied block mattress

Forces acting on a block

Limited literature is available on forces acting on blocks. According to McPherson (2015) forces acting in a block mattress are lift (F_L) and drag (F_D) forces competing against the restoring forces of gravity (F_G) and friction (F_F). Thus, the forces acting on a block can be considered similar to the forcing on a single grain.

$$F_D = \frac{1}{2} C_D A_D \rho u|u| \quad [2.6]$$

$$F_L = \frac{1}{2} C_L A_L \rho u|u| \quad [2.7]$$

$$F_G = (\rho_b - \rho)\, gV \quad [2.8]$$

$$F_F = C_F(\rho_b - \rho)\, gV \quad [2.9]$$

C_L and C_D are lifting and drag coefficients respectively, and u is the velocity near the grain. A_L and A_D are exposure areas and generally, they are related to the nominal diameter. In both cases, averaged velocity is used to determine the drag and lift forces.

However, the velocity is not constant and the fluctuations of the velocity cause fluctuations of the forces (Hoan 2008). According to Hoan (2008) the extreme values of |u'| can be in the order of magnitude as $|\bar{u}|$ so the fluctuating parts of the lift and drag forces are important on stability.

By combining equation 2.1 with [2.6] and [2.7] the instant forces will follow the next structure.

$$F_D = \frac{1}{2} C_D A_D \rho_w \, (\bar{u} + u')^2 \qquad [2.10]$$

$$F_L = \frac{1}{2} C_L A_L \rho_w (\bar{u} + u')^2 \qquad [2.11]$$

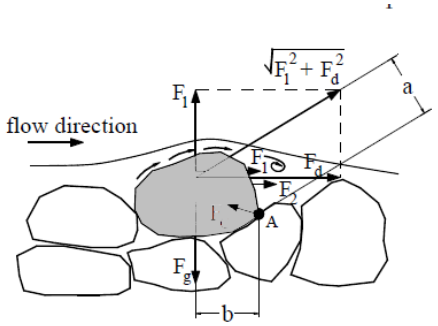

Figure 2.2: Forces acting on a particle (Hoan 2008)

The fluctuating forces generated by the same mechanism that the mean forces are known as quasy-steady forces (QSF). QSF are a consequence of the curvature of the streamlines, induced by the protruding of the particle (Hofland 2005)

By contrast, there are fluctuating forces that are also present on smooth walls. This, turbulent wall pressures (TWP) are caused by the streamwise curvature induce by turbulence.

Failure of a block mattress

Goldbold (2014) suggested that the main failure mode of the block mattresses under water flow is "edge lift". Hydrodynamic lift causes the leading corner of the mattress to be lifted sufficiently for water to flow under the mattress. Once the water flows under the mattress, the increasing on the drag forces leads to further uplift and removal. This suggestion was also made by Van Velzen and De Jong (2015) that denominated it as snow-ball effect. The different failure mechanisms (rocking of the blocks, flapping of the mattress and removal of the mattress) succeed each other rapidly and it is not possible to separate them (Van Velzen and De Jong 2015).

Moreover, several authors have suggested the importance of turbulence on the failure of block mattresses. Escarameia (1995) concluded from empirical evidence that the critical velocities for the onset of instability reduce more than 60% on highly turbulent environments. At the same direction, Goldbold (2014) asserted that mattresses that may be stable under given hydrodynamic load conditions become unstable when placed around / adjacent to a structure.

Besides, the failure of the edge of the block mat was related to the relative position. Van Velzen and De Jong (2015) concluded that there are significant differences of the critical load between an “open edge” and a “close edge”.

Hofland (2005) gave a more fundamental approach to the initiation of motion of a stone. A combination of large scale sweep motion caused by QSF that increases the drag forces and a small-scale vortex that increases the lift forces via TWP. Regarding the individual movement event for individual stones, the increased streamwise velocity at the time of movement is present more often than the small-scale cause of TWP. Therefore, even that they do not completely govern the entrainment of a stone, the QSF can be considered more important.

2.3 Existing stability formulas

Several stability formulas of block mats can be found in literature, as the proposals of Pilarczyk (2001) [2.12] or Escarameia and May (1992). [2.13].

Pilarczyk (2001)

$$\Delta D = 0.035 \frac{\varphi}{\Psi} \frac{{K_T}^2 K_h}{K_s} \frac{{\langle \bar{u} \rangle_h}^2}{2g} \qquad [2.12]$$

Where:

$\Delta = Relative\ density\ (-)$

$D = Characteristic\ dimension/thickness\ \ (m)$

$g = Acceleration\ of\ gravity = 9.81\ {}^{m}/_{s^2}$

$\langle \bar{u} \rangle_h = Critical\ vertically - averaged\ flow\ velocity\ ({}^{m}/_{s})$

$\varphi = Stability\ parameter\ (-)$

$\Psi = Critical\ Shield\ parameter\ (-)$

$K_T = Turbulence\ factor\ (-)$

$K_h = Depth\ parameter\ (-)$

$K_s = Slope\ parameter\ (-)$

K_h is a parameter that relates the depth averaged velocity to the velocity at the top of the revetment, for shallow water and rough flow $K_h \approx 1$ (Pilarczyk 2001). Pilarczyk (2001) proposed values for $\Phi = 1.0$ for the edge of the mattress and 0.5 for middle of the mattress, $\Psi = 0.07$ for block mattress and ${K_T}^2 = 2$ for hydraulic jumps

Escarameia

$$\Delta D_{n50} = C \frac{V_b^2}{2g} \qquad [2.13]$$

Where:

$$C = \begin{cases} 0.36 & for\ TI < 10\% \\ 12.3\ TI - 0.87 & for\ 10\% < TI < 30\% \end{cases}$$

$$TI_u = r_u = \frac{\sqrt{\overline{(u'^2)}}}{\bar{u}} \qquad [2.14]$$

In both cases, there is a coefficient that considers the effect of turbulence, as an amplification factor of the mean velocity. In case of equation 2.12, Pilarczyk (2001) only provide values for turbulence in a qualitative aspect regarding the turbulence level: From $K_T^2 = 1$ for uniform flow to $K_T^2 = 4$ for jet flow with high turbulence intensity. However, in PIANC (2015) it is recommended that if it is possible, the turbulent factor should be derived from equation [2.15] proposed by the Rock Manual (2007). This equation presents a relation between the turbulence relative intensity and the turbulence factor.

$$K_T = \frac{1+3r}{1.3} \qquad [2.15]$$

Smyrnis (2017) proved that Pilarczyk equation does not described accurately the effect of turbulence on block mattress stability.

Escarameia and May (1992), equation 2.8, provide a relation of turbulence relative intensity and the value of the multiplying coefficient.

The correction factors are rather arbitrary, so the expression can be only used as rule of thumb or with large safety factors. The turbulence factor should be chosen according to an 'engineering judgment' (Hofland 2005). Moreover, there are several situations where the ratio of mean and fluctuation changes and the stability cannot be predicted, clear example on the reattachment point.

On the other hand, there are present in literature stability parameters that include the turbulence intensity as an addition factor to mean velocity. In this second group, it can be found the proposals of Jongeling et al. (2003), Hofland (2005) and Hoan (2008) where the turbulent is included as follows:

$$\langle \left(\bar{u} + \alpha\sqrt{k}\right)^2 \rangle_L \qquad [2.16]$$

Jongeling et al:

Jongeling et al. (2003) developed a method that derive damage on bed protections based the outputs of numerical computations. The flow loads are quantified by a combination of velocity and turbulence distributions over a certain water column above the bed.

$$\Psi_{WL} = \frac{\langle \left(\bar{u}+\alpha\sqrt{k}\right)^2 \rangle_{hm}}{\Delta g d} \qquad [2.17]$$

K is total kinetic energy, α is an empirical turbulence magnification factor, $\langle \dots \rangle_{hm}$ is a spatial average over a distance of hm above the bed. Ψ_{WL} is based on values of α and hm. First, experiments for various flow configuration at incipient conditions were done.

Second, experiments were simulated by numerical flow models. Finally, after comparison of the various geometries, α=6 and hm = 5d + 0.2h were proposed.

The main advantage is that the turbulence is explicitly modelled. However, the method of choosing α and hm is questionable because there is not proof that critical stability parameter must be a constant value. As pointed by Hofland (2005), using a subjective incipient motion will not yield consistent design criteria. Jongeling defined the incipient motion by visual observation method. Therefore, the link between $\Psi_{WL,c}$ and the stability state of bed material is not clear.

Hofland

Hofland (2005) derived a method for stability of bed protections under non-uniform flow based on the outputs of a 3D RANS model. The loading forces are quantified by the combination of the profiles of velocity and turbulence. The maximum over the depth of the local values of $(\bar{u} + \alpha\sqrt{k})$ weighted with the relative mixing length L_m/z was used.

$$\Psi_{Lm} = \frac{\max\left[\langle \bar{u} + \propto\sqrt{k}\rangle_{Lm}\frac{Lm}{z}\right]^2}{\Delta g d} \qquad [2.18]$$

Where Lm is Bakhmetev mixing length ($L_m = \kappa z\sqrt{1-\frac{z}{h}}$) that is a moving average with varying filter length Lm, and z is the distance from the bed. An analysis based on data of Jongeling et al. (2003) and De Gunst (1999) was done. From the analysis α = 6 fits best with the data.

Hoan

Hoan (2008) also derived a stability equation where the acting forces are the mean flow velocity and the turbulence intensity. However, instead of using the Bakhmetev mixing length, he proposed to average the velocity and the turbulence over the whole depth but combined with a weighting function. The weighting function accounts a maximum influence of turbulence near to the bed that decreases over the water column.

$$\Psi_{u-\sigma[u]} = \frac{\langle[\bar{u} + \alpha_T\sigma\,(u)]^2\left(1-\frac{z_b}{h}\right)^{\beta}\rangle_h}{\Delta g d} \qquad [2.19]$$

In those cases, the instability is based in a combination of velocity and turbulence intensity averaged over a certain water depth. The selected water depth and the value of α as an amplification factor varies on the different proposals. The temporal maximum of the local velocity is quantified as the mean velocity plus few times the turbulence intensity. In case of Jongeling (2003) and Hofland (2005), turbulence was included as the total kinetic energy, while Hoan (2008) only considered fluctuations in stremawise direction.

Other authors like Steenstra (2014) researched the stability parameter in non-uniform flows by adding the forces caused by the pressure gradient due to quasi steady forces. However, in any further research the stability under non-uniform flows of block mattresses has been studied.

Stability equations based on shear stresses (see Shields 1936 or Grass 1970) have not been considered at the study. Hoan (2008) proved that the use of bead shear stress to quantify the flow forces are insufficient for non-uniform flow due to the lack of combination of velocity and turbulence.

2.4 Conclusions

In this section, the most important aspects of the stability of block mattresses under non-uniform flow are summarized. The objective of this literature review is to establish the foundation in which the development of a new stability equation for block mattresses will be based.

First, different expressions used to determine the turbulence as the fluctuations of the instant flow velocity over the mean velocity were checked. Even that fluctuations are chaotic and irregular motions, different statistical parameter can describe them (Schiereck 2012). Moreover, the flow patterns follow certain structures that can be related to initiation of motion (Hofland 2005).

The turbulence intensity will be increased at the flow by the presence of a weir upstream of the block mattress. Weirs are common hydraulic structures that generate a high amount of turbulence downstream (Gharahjeh, Aydin and Altan-Sakarya, 2015). However, there is not any previous work that relates their presence with the instability of block mattresses downstream.

Block mattresses are broadly used bed protections, which are form by the combination of a geotextile and concrete blocks. The forces acting on a block mattress are the drag and lift forces (McPherson 2015). Although the average velocity is used to compute the forces values, the fluctuations forces caused by the flow fluctuations should be carefully studied and related to initiation of motion (Goldbold 2014). Besides, quasy-steady forces and turbulence wall pressures are also acting on the blocks (Hofland 2005).

Block mattresses failure is related to the edge lifting that leads to the total removal of it (Van Velzen and De Jong 2015). The failure is sudden and unstoppable once has started. It has been proved by several authors the reduction of stability due to turbulence (Goldbold 2014 and Escarameia 1995). Moreover, it has been concluded that the stability is related to the relative position of the edge of the mattress (Van Velzen and De Jong 2015).

The stability equations available in literature (Pilarczyk 2001 and Escarameia 1992) for block mattresses are based in mean velocities and turbulence is included as an amplification factor. However, there are several situations where the ratio between mean and fluctuating velocity changes, like the reattachment point (Hofland 2005). Moreover, Smyrnis (2017) proved that Pilarczyk equation does not predict the stability of block mattresses under non-uniform flow.

In a different approach, Jongeling (2003), followed by other authors like Hofland (2005) and Hoan (2008), derived a new stability parameter considering the maximum forces as a function of the mean velocity plus few times the standard deviation. These equations were derived for rip rap bed protections. However, they proposed a new alternative to consider velocity fluctuations that can be useful at the present study.

3. Experimental arrangement

3.1 Introduction

The objective of this thesis, as mentioned on section 1.2 is to study the stability of block mattresses under non-uniform flow. Due to the lack of available data, more experiments are needed to follow the work started by Smyrnis (2017). Thus, it is expected that the obtained data provide relevant information to investigate the failure modes induced by a high turbulent flow.

For this purpose, different combinations of mean velocity and turbulence intensity were studied. Four configurations, two heights and two distances downstream of the structure, were studied to check different combinations of mean velocity and turbulence intensity at failure moment.

In this chapter, all the relevant information relative to experimental arrangement and configuration is present. The experimental configuration, the expected scale effects, the test programme and the selected time series are given.

3.2 Experimental configuration

The tests were carried out in an open-channel flume in the Fluid Mechanics Laboratory of the department of Hydraulic Engineering of the faculty of Civil Engineer, Delft University of Technology.

This set of tests act as a continuation of the works done by Van Velzen and De Jong (2015) and Smyrnis (2017)

The flume

The selected flume characteristics are summarized in figure 3.1. The flume is 14 m long and 0.4 m wide. The maximum allowed water depth is 40 cm and the maximum flow discharge is 60 l/s. The same flume was used by Smyrnis (2017) at the previous step of the study.

Figure 3.1 shows elements configuration. Those are the parameters changing in the different configurations.

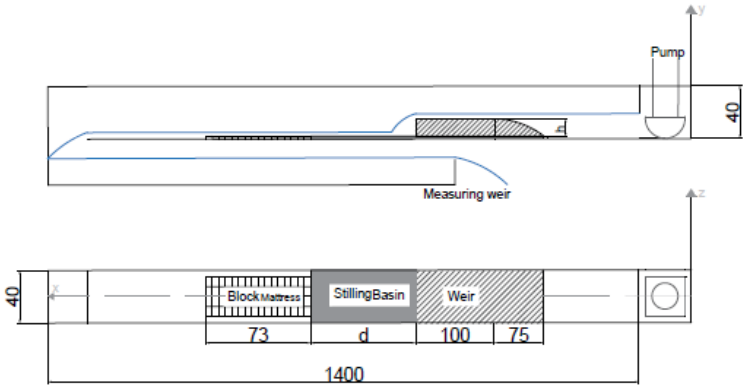

Figure 3.1: General view of the flume and the elements configuration. Note that the figure is not at scale and that the distances are in cm. The height of the weir (h) and the length of the stilling basin (d) are not defined on the general view.

Description of the set up

During the experiment set-up, particular care was taken to ensure the two-dimensional behaviour of the flow. For this purpose, the connections with the side wall were made water tight to avoid any interfere with the flow over the weir. Moreover, the front part of the apron was made water tight by adding a piece of wood and gluing the connections. This measure was important because the impact of the infiltrate water would reduce the stability of the block inducing large scale effects.

Figure 3.2: Detail of the transition between the stilling basin and the block mattress

- *Block mattress*

The block mattress is form by sixty concrete blocks distributed in fifteen rows of four blocks. The connection between the blocks and the geotextile is achieved by glue and screws, with two screws per block. The total dimension of the mattress are 742.5mm length and 306mm wide (See annex 2 for more details).

The concrete blocks dimensions are summarized in figure 3.3. The density of the material according to the supplier is 2312 kg/m^3.

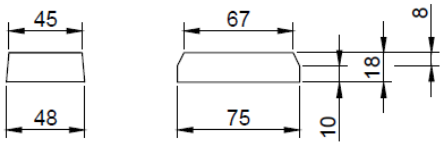

Figure 3.3: Detailed dimensions of the blocks. Dimensions in mm

The used geotextile is a PP15 geotextile of Ten Cate Geolon made of polypropylene tape and split fibre yarns. The geotextile properties are summarized in table 3.1.

Properties	Value	Unit
Tensile strength	16	kN/m
Elongation at min strength	17	%
Static puncture resistance	2,3	kN
Dynamic perforation	19	mm
Permeability	12	mm/s
O_{90}	250	µm

Table 3.1: Properties of the geotextile according to the information provided by the supplier

Instrumentation

In the experiment, there are four relevant parameters that should be measured: the water velocity signal, the discharge, the failure of the block and the water depth. Each of them has different technical requirement that should be analysed:

- *Velocity signal:*

For the development of the thesis, the measurement of the velocity signal is a key aspect. The selected device should have enough accuracy and the sampling frequency to measure the turbulence fluctuations of the flow. Moreover, the device should minimize the disturbance of the flow. There are different devices that can be used to measure velocities:

- Acoustic Doppler Velocimeter (ADV)
- Laser Doppler Velocimeter (LDV)
- Particle Image Velocimeter (PIV)
- Electromagnetic Flow Meter (EMS)

Different devices have their strengths and their limitations. Electromagnetic Flow Meter, used by Smyrnis (2017) to measure flow at the experiments, is a simple device based on Faradays induction law. After a good calibration, the electronics allow to measure with a maximum frequency of 10 Hz, what allows enough resolution to measure mean velocities and the fluctuation of the large-scale turbulence.

Particle Image Velocimeter is a device that allows to visualize the spatial structure of the flow and relate it to the failure of the bed protection. The measurements are based on a laser beam longitudinal to the flow from which the velocity vectors can be derived. Hofland (2005) concluded, based on PIV, that the most unfavourable situation for stability is when the size of the eddy is comparable to the size of the stone. By contrast, the equipment needed to measure and process flows measured with PIV is complex and expensive.

The Acoustic Doppler Velocimeter provides a three-component velocity based on the frequency shift between the emitted acoustic wave and the received one. The Doppler shift can be related to the instant velocity with high measurement frequency (Song and Chiew, 2001). Although the ADV has its limitations (García et al., 2005) based on the combination of sample frequency, water depth and flow velocity and the effect of white noise, the ADV has been probed to measure the vertical component of velocity accurately (Voulgaris and Trowbridge, 1998). However, the ADV needs to be placed inside the water and the measured volume is placed 5 cm from the device. It is expected that in several test situations the water depth is small and furthermore, the disturbance of the ADV at the flow should be avoid.

Laser Doppler Velocimeter is a popular device to measure turbulence effect, used by Hoan (2008), which provides a high accuracy without interrupting the local flow. The flow velocity is measured by sending two coherent lasers beams that intersect in a certain control volume. The particle that passes the control volume will scatted the light with an attained Doppler shift that can be related to particles velocity. LDV provides accurate measures of fluid particles that make it an excellent device to measure turbulence. Therefore, LDV is the most suitable device to measure water instant velocity and it was selected for the measurements during the tests.

For the present study, a 400mm lens was used, which results in a measuring volume of about 10mm in spanwise direction and 1mm in the other directions. The sampling frequency was limited by the sampling frequency as it is discussed in the next section. The sampling water volume was placed at the middle to the flume and 5mm above the block mattress.

The calibration of the velocity signal was done according conversion factor for a Lens type of 400 mm of 7.4 V/m/s to transform the voltage into velocity signal. Moreover, signal was transported from A and B beams to horizontal and vertical velocity (Figure 3.4) leading to equations [3.1] and [3.2]

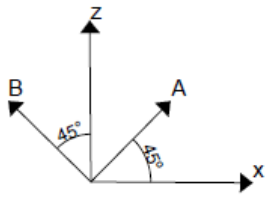

Figure 3.4: Axes transformation between the LDV signal and the velocity signal. Note that A and B are the measuring axes of the LDV and x and z the horizontal and vertical axes of the flume

$$u = A\frac{1}{7.4}\frac{\sqrt{2}}{2} + B\frac{1}{7.4}\left(-\frac{\sqrt{2}}{2}\right) \quad [3.1]$$

$$w = A\frac{1}{7.4}\frac{\sqrt{2}}{2} + B\frac{1}{7.4}\left(\frac{\sqrt{2}}{2}\right) \quad [3.2]$$

- *Failure of the block*

To record the failure moment of the block, a high-speed camera synchronized with the LDV recorded time series was used. The sample frequency of the high-speed camera was an important limitation for the test. The use of an external trigger for the camera was not working for sampling frequencies higher than 20 Hz. Because of this limitation, the LDV sampling frequency was fixed at 80 Hz, thus, four measures were obtained for each frame of the camera. The failure moment was defined as the displacement of the block higher than half of the block thickness (1cm). The use of accelerometers was rejected due to the lack of time to fix them to blocks without disturbing the flow. However, this option should be studied in further researches.

- *Water level*

The water level is a relevant parameter to compute important flow properties as the Reynolds and the Froude number. After trying to measure the water depth with laser it was concluded that most accurate device to measure the water level was by a tapeline and visual observation. The fluctuation of the water surface limits the accuracy of the measurement to 5 mm.

Measurement	**Velocity**	**Discharge**	**Failure**	**Water level**	**Distance downstream**
Measurement equipment	LDV	Display + weir	Camera	Tapeline	Tapeline

Table 3.2: Summary of measurements equipment

- *Discharge measurement*

The discharge was measured by recording the display of the water pump. However, the displayed discharge has a deviation from the real value. The flume is equipped with a well calibrated measurement weir. The water level is related to the discharge by the rehbock equation (annex 3). As the water level at the measuring weir needs at least 15 minutes to be accurate, a series of test of 20 minutes were done, where both values (display and weir height) were measured and thereafter, a table of conversion values was derived. For both devices, lineal transformations were done to calibrate the electric power.

Pipe discharge [l/s]	Water depth [cm]	Real Discharge [l/s]	Error [%]
3,9	30,8	4,57	14,66
6,8	43,8	7,68	11,46
10,7	58,3	11,77	9,09
14	69,9	15,47	9,50
16,9	78,8	18,55	8,89
17,7	81,1	19,38	8,67
18,9	84,9	20,78	9,05
21,9	93	23,88	8,29
22,7	95,1	24,71	8,13
24,1	98,8	26,2	8,02
26,8	106,1	29,23	8,31
28,3	109,6	30,37	6,82
31,2	117	33,99	8,21
33,1	121,3	35,94	7,90
34,3	124	37,19	7,77
36,5	129,1	39,588	7,80
37,9	132,3	41,12	7,83

Table 3.3: Conversion values for the discharge measuring

The failure of the block mattress is a required event for the development of the thesis. Consequently, the flow generated forces acting on the blocks must be enough to induce failure. The same flume and block mattress were used in Smyrnis (2017), where several failures were achieved over a range of different mean velocities and turbulence intensities. Thus, it can be expected that the flow conditions will induce failure and relevant conclusions can be derived from the tests.

3.3 Scaling

Prototype scaling

Physical hydraulic modelling is a common tool for finding technically and economically optimal solutions for hydraulic engineering problems (Heller 2011). However, considerable differences can arise between the scaled model and the prototype, scale effects. In general, the scale effects or disturbance increase with the scale ratio or scale effect:

$$\lambda = \frac{L_p}{L_m} \quad [3.3]$$

Where L_p is the characteristic length of the prototype and L_m the one from the model. Hughes (1993) (in Heller 2011) pointed that this definition of scale ratio is not universal and sometimes it is defined as the inverse.

A physical scale model is completely similar to its real-world prototype and involves no scale effects if it satisfies mechanical similarity implying the Geometric, kinematic and Dynamic similarities (Heller 2011).

The Dynamic similarity implies that Geometric, kinematic and all forces ratios in two systems are identical. The inertial force is normally the most relevant in fluid dynamics and it is, therefore, included in all common forces ratios. For the scope of the thesis the Froude and Reynolds similarities will be specified.

Froude similarity is the most applied criterion applied in open-channel hydraulics. It is especially suited for model with turbulent phenomena since the energy dissipation of the latter depends mainly on the turbulent shear stress. Under Froude similarity, the remaining forces ratios cannot be identical between model and real-world prototype and may therefore result in non-negligible scale effects (Heller 2011).

Reynolds similarity is relevant for seepage flows, creeping flows around spheres or particularly at boundaries resulting in excessive losses in a model compared to the prototype. It is important that the flow regime does not change between prototype and model (Heller 2011).

Scaling of the mattress

At the present study, the flow and structure configurations do not follow a real-world prototype similarity. However, the Froude and Reynolds similarity can be applied to fix the range of use of the derived stability equation. Nevertheless, the model mattress is based on the GS-VB-15 produced by Holcim Coastal BV with a prototype thickness of 150mm, corresponding to an approximate scale ratio of 8.

Some differences are present between the GS-VB-15 and the tested mattress that should be considered. The connection between the geotextile and the block is achieved by pouring the concrete over the geotextile. At model scale this is not possible, so the connection is achieved by glue and screws.

The density of the model is slightly different from the prototype. When the concrete is poured in small quantities, the density is likely to be smaller because the pebbles/fillers are included in the same amount. Holcim concluded that the density of the model is 2312 kg/m^3 while the prototype's density is 2350kg/m^3.

Additionally, to ensure the feasibility of the model block fabrication, some simplifications of the shape were done as can be observed in figure 3.5. These simplifications do not have considerable effects on the stability of the block mattress.

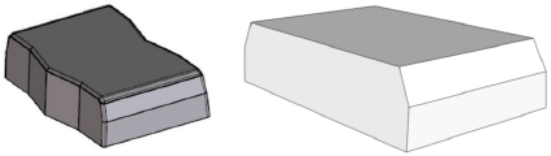

Figure 3.5: Shape difference between prototype and model blocks, Van Velzen and De Jong (2015)

Scale effects

Despite that the similarity conditions can be achieved in most of the variables, Van Velzen and De Jong (2015) pointed several scale effects on their analysis of the stability under propeller flow. Special attention in payed to two aspects of the geotextile, the stiffness and the permeability.

However, even that the most flexible geotextile was chosen for the model mattress, it was still too high. The stiffness of the material is a relevant parameter on the resistance against local flapping. Thus, the model will have an extra resistance due to the stiffness of the geotextile. According to Van Velzen and De Jong (2015), the contribution of the geotextile to the resistance against overturning is 7% at the model while at the prototype is around 0.03%.

Moreover, the permeability has also influence on the stability of the block mattress. A more impermeable geotextile at the model leads to a higher resistance at the middle of the mattress. By contrast, a more impermeable model geotextile is more unstable at the edges of the mattress. Considering that the edges are the most critical parts of the mattress, a conservative decision was taken by choosing a more impermeable geotextile at the model.

3.4 Test programme

The tests configurations followed in this thesis have two different components; the height of the weir and the distance between the weir and the block mattress. Two different heights were studied (15 and 18,5 cm) and two different distances for each height, in both cases 3h and 4h. These distances were checked based on the quality of the obtained data, influenced by the interaction of air bubbles on the water with the LDV.

Two different series of test were carried. In the first series, four failures for each of the configurations were recorded for a total of 16 failures. In all the failures, the procedure to follow was the same:

1. Open the valve at a low discharge value.
2. Once the discharge is constant, record a series of 2 minutes each.
3. Increase the discharge (The increases of discharge were around 1 l/s).
4. Once the discharge is constant, record a series of 2 minutes each.

Thereafter, a data base was done to derive accurate mean velocity and turbulence intensity for each configuration. During the data base, discharges larger than the failure one were

recorded. The failure of the blocks disturbs the flow, modifying the flow properties. To avoid this disturbance, the last block row was glued to the previous row. A total of 54 series were recorded to complete the database. At chapter 4, the all the details of the failures are mentioned. Moreover, in chapter 5 the failures are combined with the data bases to derive a stability equation.

Configuration	number of steps	Initial discharge	Final discharge
1	10	17	19
2	15	13.4	15,7
3	11	11,75	15
4	18	10	20

Table 3.4: Summary of the data base steps

3.5 Data processing methods

The velocity data collected from the data was used to compute the characteristics of the flow. Two different kind of parameters were differentiated. First, the statistical parameters were derived from the measured time series and the properties of the flow characterized. Second, the failure velocity was obtained by the synchronized use of the LDV and the movement sensors. In chapter 5, the relation between the critical velocity and the flow properties, as a combination of mean velocity and turbulence fluctuations, is analysed.

The flow conditions from the different test were described by time series obtained from the measurements. The mean velocity was derived as follows:

$$\bar{u} = \frac{1}{N}\sum_{i=1}^{N}(u_i) \qquad [3.4]$$

Where N is the number of samples. From the mean velocity, the velocity fluctuations were obtained as:

$$u' = u_i - \bar{u} \qquad [3.5]$$

As has been previously mentioned, the turbulence intensity is defined as:

$$\sqrt{\overline{(u')^2}} = \sigma_u = \sqrt{\frac{1}{N}\sum_{i=1}^{N}(u_i - \bar{u})^2} \qquad [3.6]$$

Note that the turbulence intensity only considers the fluctuation at the streamwise direction. Hofland (2005) pointed that the fluctuations on the vertical direction have also and influence on the initiation of movement. Thus, the total kinetic energy was defined as:

$$k = \frac{1}{2}\left(\overline{(u')^2} + \overline{(v')^2} + \overline{(w')^2}\right) \qquad [3.7]$$

As aforementioned, the failure velocity was compute as a combination of mean velocity and a turbulence parameter. The decision of define turbulence as the fluctuations of the streamwise direction, as a combination of u' and w' or as the total kinetic energy is discussed at chapter 5.

The measurement of the velocity signal by the LDV was only recorded in streamwise and vertical directions. Thus, the velocity signal in y-direction was not obtained. Based on the empirical factors of standard deviation given by Nezu and Nakagawa (1993) (In Steenstra 2014) and the analysis of turbulence statistics of Kim, Moin and Moser (1987) the turbulence intensity in y-direction was assumed to be equal to turbulence intensity in upwards direction. Hoan (2008) solved this problem by measuring the relation of standard deviation in streamwise and transvers direction by a EMS. He concluded that:

$$\sigma_v = {}^{\sigma_u}/_{1.9} \qquad [3.8]$$

To compare the results, the ratio between standard deviation of *u* and *w* was done for the measured time series, obtaining a value of 1.8 (see annex 4). Thus, the obtained results validated the previous assumption.

The failure of the block mattress was process by the analysis of the camera frames. Based on the visual confirmation of the failure, the associated time step was chosen. The signal length of the failure was considered 1.5s before the failure to provide a larger scale frame of the velocity signal. The data of the signal after the failure was not available in several failures due to obstruction of the lifted block on the laser beam.

3.6 Selected time series

To conclude the signal length for each of the measurements, the accuracy of different duration was checked. The relevant data obtained from the signal was mainly the streamwise velocity, the streamwise turbulent intensity and the total kinetic energy. The duration of the signal should be long enough to describe accurately the statistical parameters, but at the same time not too large to optimize the efficiency of the tests.

With this purpose, a signal was measured for 30-minute duration. The mean velocity, the standard deviation in streamwise direction and the total kinetic energy were determined. These values were used as a reference value for estimating the errors of the shorter measuring lengths. From the original signal, 50 series were selected randomly of a duration of 2, 5 and 10 minutes. Then, the obtained statistical values were computed with the reference values by using equation [3.9].

$$\delta_x = \frac{x - x_0}{x_0} \times 100 \qquad [3.9]$$

Where x is the values of the series and x_0 is the reference value. Figure 3.6 showsthe obtained results.

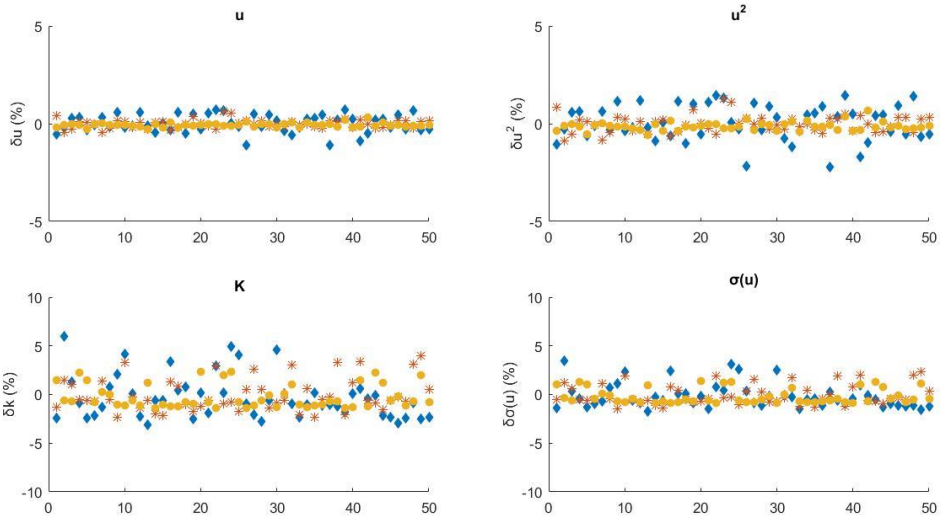

Figure 3.6: The relative errors of 2 minutes(diamonds), 5 minutes (stars) and 10 minutes (circles)

Based on the results, a duration of two minutes was chosen. The relative errors were smaller than 5% for all the parameters and the improvement of results for the duration of 5 minutes was not enough to justify the larger measurement duration.

4. Failure mechanism

4.1 Introduction

The failure of the block mattress during the test series was located at the last row of blocks. To understand the processes and mechanisms inducing the failure the flow structures and the behaviour of the blocks were studied. Failure was defined as a displacement larger than half of the block thickness (1cm). This study was divided in two different sections. In the first one, the flow associated to the failure was studied and in the second one, the weakness of the last row was studied. In this chapter, all the information related to the failure of the mattress is analysed.

The chapter is composed as follow. Section 4.2 describes the flow parameters at the failure. The flow structures leading to failure are studied in section 4.3. This is followed by the analysis of the flow over the last row in section 4.4. Finally, the chapter ends by the summarizing conclusions and a proposed last row block shape in section 4.5.

4.2 Flow characterization

The previous chapter described the 16 failures recorded during the experimental phase of the study. The failure instants were obtained by synchronizing the camera frames with the velocity signal. The camera sampling frequency was 20 Hz while the velocity signal was 80 Hz. Thus, the accuracy of the failure instant is 0.05s. Table 4.1 summarizes the flow parameters of the failures.

Measured flow parameters

Failure	Configuration	h_{weir} [cm]	d_{basin}	$Q_{measured}$ [l/s]	U_{fail} [m/s]
1	1	18,5	3h	18,02	1,55
2	1	18,5	3h	17,57	1,45
3	1	18,5	3h	17,70	1,49
4	1	18,5	3h	17,76	1,64
5	2	18,5	4h	14,86	1,46
6	2	18,5	4h	14,55	1,47
7	2	18,5	4h	14,68	1,56
8	2	18,5	4h	14,52	1,56
9	3	15	3h	13,12	1,60
10	3	15	3h	13,51	1,43
11	3	15	3h	12,96	1,57
12	3	15	3h	12,37	1,59
13	4	15	4h	17,73	1,68
14	4	15	4h	17,75	1,68
15	4	15	4h	16,57	1,52
16	4	15	4h	17,29	1,65

Table 4.1: Summary of the measured flow parameters on the failures Note that U_{fail} is the peak of velocity found in the velocity signal associated to the failure of the block. $Q_{measured}$ is obtained by the measurements at the pump pipe.

Calculated flow parameters

As mentioned in chapter 3, the measured discharge had an error that was solved by using a conversion table (See annex 2). The real discharge was computed based on the measured discharge and the conversion table.

Moreover, with the calculated discharge and the measured water depth (h) during the experiments, some flow parameters were computed:

$$U = \frac{Q}{Bh} \quad [4.1]$$

$$Re = \frac{Uh}{\nu} = \frac{Q}{B\nu} \quad [4.2]$$

$$Fr = \frac{U}{\sqrt{gh}} = \frac{Q}{Bh\sqrt{gh}} \qquad [4.3]$$

In chapter 3, the scale similarities based on Reynolds and Froude number have been mentioned. Even though the present study does not follow any prototype, both Reynolds and Froude number provide information about the flow. Additionally, they define the range of conditions where the tests were done.

Failure	Qfail [l/s]	Qreal [l/s]	h [m]	Uave [m/s]	Re [10^4]	Fr [-]
1	18,02	19,75	0,04	1,23	4,89	1,97
2	17,57	19,25	0,04	1,20	4,76	1,92
3	17,70	19,37	0,04	1,21	4,80	1,93
4	17,76	19,45	0,04	1,22	4,81	1,94
5	14,86	16,38	0,035	1,17	4,05	2,00
6	14,55	16,06	0,035	1,15	3,97	1,96
7	14,68	16,19	0,035	1,16	4,01	1,97
8	14,52	16,02	0,035	1,14	3,96	1,95
9	13,12	14,49	0,025	1,45	3,59	2,93
10	13,51	14,93	0,025	1,49	3,69	3,01
11	12,96	14,30	0,025	1,43	3,54	2,89
12	12,37	13,64	0,025	1,36	3,38	2,76
13	17,73	19,42	0,03	1,62	4,81	2,98
14	17,75	19,44	0,03	1,62	4,81	2,99
15	16,57	18,20	0,03	1,52	4,50	2,80
16	17,29	18,96	0,03	1,58	4,69	2,91

Table 4.2: Summary of calculated flow parameters

Reynolds shear stress

According to Hoan (2008) and as it was mentioned in chapter 2, shear stress does quantify sufficiently the flow forces for non-uniform flow due to the lack of combination of velocity and turbulence. However, Reynolds shear stress [4.4] provide information about the coherent structures of the flow.

$$\tau_{xz} = -\overline{u'w'} \qquad [4.4]$$

In Hofland (2005) the initiation of motion of a single stone was related to a combination of an increase in vertical velocity (Burst) followed by an increase in streamwise velocity (Sweep), both related to positive Reynolds shear stresses.

4.3 Failure structures

In this section, the coherent structures leading to the failure of the block mattress are studied. During the tests, it was realized that the failure could be related to the addition of two different processes, an increase of the exposure area and the lifting of the block. Unlike the initiation of motion in a single stone, in the movement of a block, both episodes were spread in time.

Increase of the exposed area

In chapter 2, the forces acting on a single block were derived. Equations 2.10 and 2.11 show that the forces (lifting and drag) are proportional to the exposure area of the block. Thus, if the block is initially shielded by other blocks, an initial lifting seems to be an essential process to initiate the motion.

Figure 4.1: Increase of exposure area of the block

Figure 4.1 shows that the last row of block is slightly lifted and that part of the front face of the block is exposed to the flow. Unfortunately, it was impossible to relate the initial lifting of the block by synchronizing the camera with the velocity signal. However, according to Hofland (2005), this movement can be related to Turbulent wall pressures(TWP).

In turbulent flow, pressure differences due to the streamline curvature are always present, also in smooth beds. In figure 4.2, the effect of a passing vortex in a stone is shown. The effect of the passing vortex it is expected to be similar over a block

Hofland (2005) concluded that for stones shielded by other stones, the TWP are important for the movement of a stone. Moreover, the influence of TWP seems to be larger on the lifting forces than on the drag forces. The TWP themselves lead to an upward-downward motion of the stone.

At the present study, it was observed that initially shielded blocks were lifted increasing the exposure area. Without the possibility to synchronize the movement to the velocity, previous related studies were studied. Thereafter, it can be concluded based on Hofland (2005) that the TWP play the key role on the initial lifting of the block.

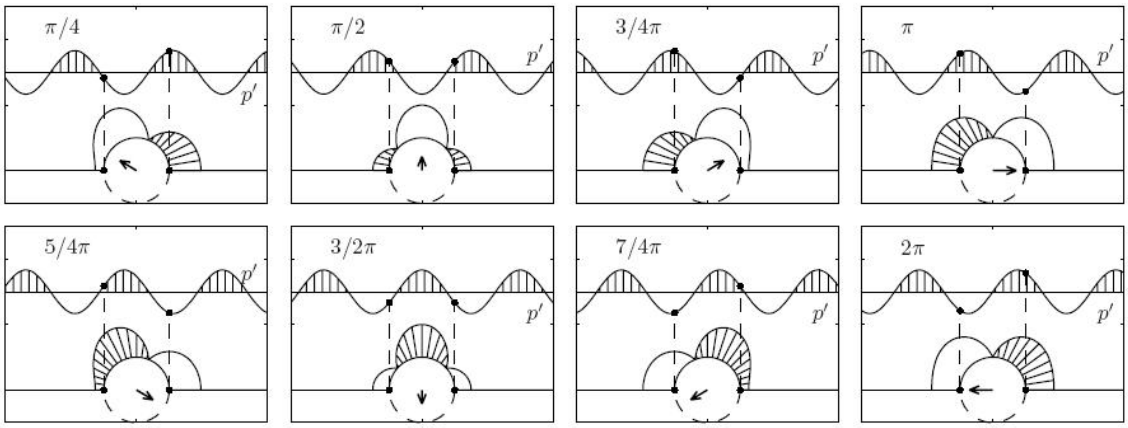

Figure 4.2: Change of the integrated force on a stone. The vectors represent the resulting net force acting on the stone (Hofland 2005)

Although the last row of blocks was slightly lifted and the exposure area was increased, the mattress was still stable. Therefore, some other structures should be acting on the blocks to induce failure.

Failure of the block mattress

The increase of the exposed area of the block is a required step on the failure of the block, however, it is not the most relevant one. Table 4.3 summarizes the frame where failure was defined and the associated time. The failure of the block was defined as a displacement larger than half of the block thickness (1cm).

The movement of the block showed fluctuations of displacements before failure. However, the block moved back to the initial position. 1 cm was proved to be an accurate threshold of failure, because after displacements larger than half of the block, the blocks were not able to move back to initial position. This failure, by contrast, was not followed by a total removal of the whole mattress as could be expected from previous literature Goldbold (2014). Figure 4.3 shows the last row position after the failure.

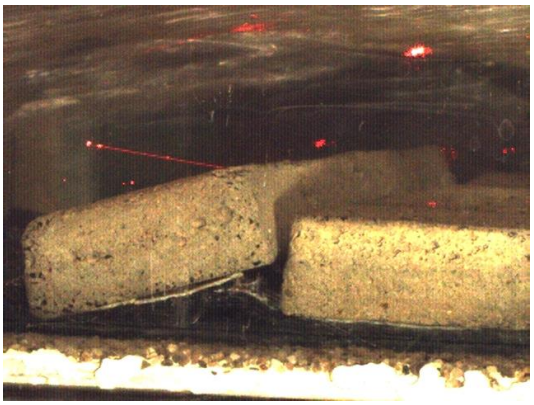

Figure 4.3: Failure of the last row of the block mattress

Failure	Frame	t [s]
1	3055	152,75
2	2745	137,25
3	3716	185,8
4	5782	289,1
5	690	34,5
6	586	29,3
7	770	38,5
8	774	38,7
9	664	33,2
10	1483	74,15
11	915	45,75
12	730	36,5
13	256	12,8
14	1826	91,3
15	783	39,15
16	1518	75,9

Table 4.3: Summary of the failure frames and associated times

The velocity signal provides relevant information related to the coherent structures of the flow. Figure 4.4 shows the signal of the last 1.5s before the failure for four randomly chosen series, one for each configuration (See annex 5 for the rest of the failures). The four samples of the signal have a peak of streamwise velocity near the failure.

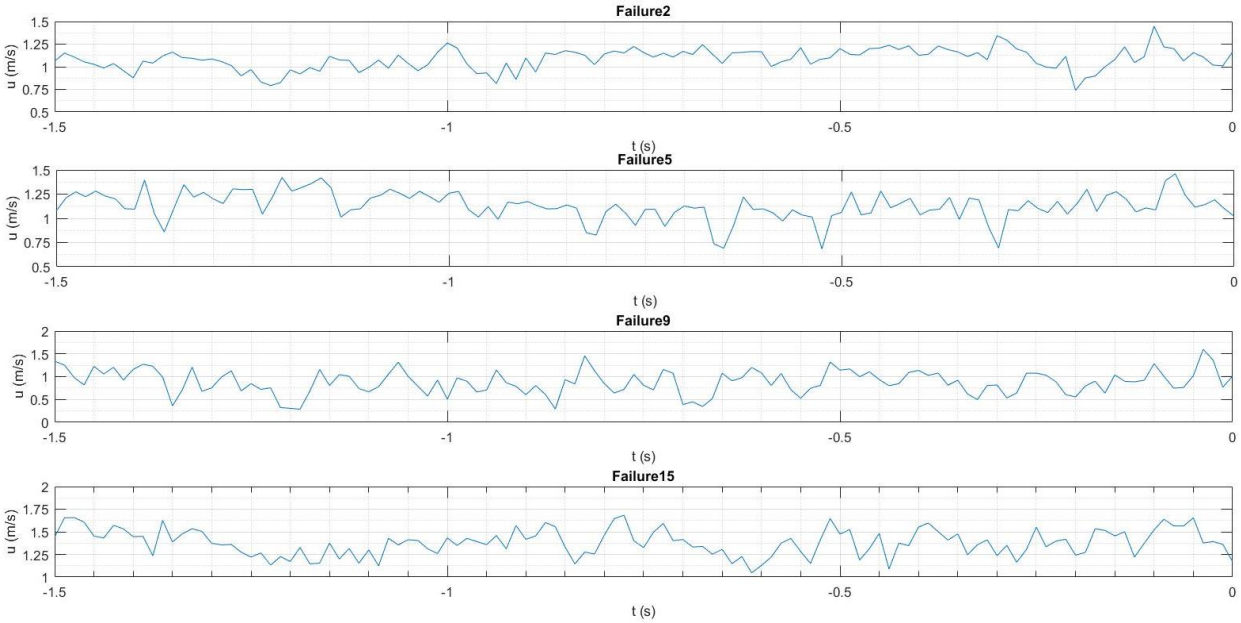

Figure 4.4: Time series of 4 failures, for the different configurations. The failure instant is located at time 0 to synchronize failures

To provide a clearer vision of the failure mechanism, figure 4.5 shows an ensemble averaging of the 16 failures. The averaged velocity shows a clear peak of velocity close to failure. Moreover, the coloured areas show that the results are spread over the mean.

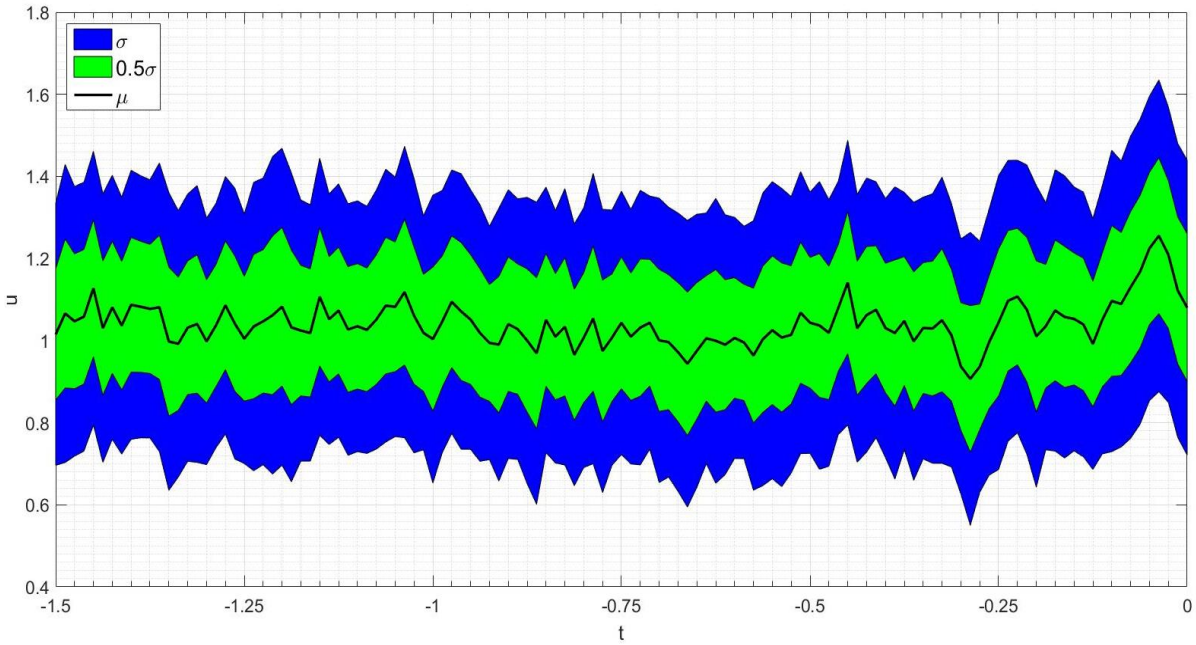

Figure 4.5: Ensemble averaging of the failure velocity signal. The coloured areas show the spread of the sample by the standard deviation

By also considering the vertical velocity signal and the shear stress, both averaged over the sixten failures, the failure mechanism can be indentied as a sweep. An increase in streamwise velocity, combined by a downward vertical movement leading to an increase in shear stress (Q4). Moreover, figure 4.6 also show that Q2 and Q4 event are more frequent peaks of shear stress than the Q1 and Q3 events as should be expected.

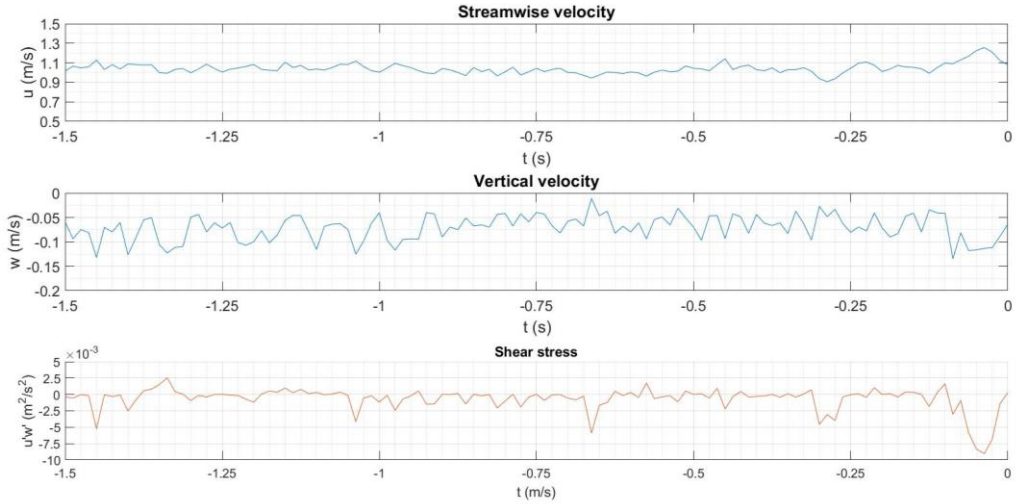

Figure 4.6: Ensemble averaged signal of the streamwise velocity (u), vertical velocity (w) and Reynolds stresses (u'w')

The failure of the block mattress, thus, is caused mainly by a peak of fluctuation at the streamwise velocity. This finding matches with the assumption the maximum forces are proportional to the addition of fluctuations to the mean velocity [4.5].

$$F_{max} \propto \rho(\bar{u} + u')^2 d^2 \qquad [4.5]$$

However, the signals show that before the failure, combinations of higher streamwise velocities and Reynolds stresses were present in some of the failure signals.

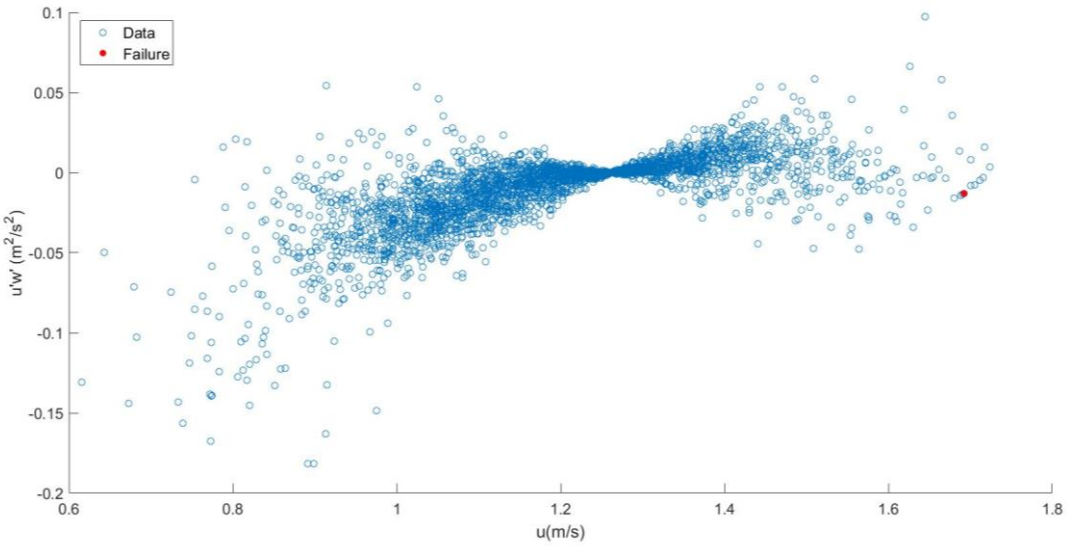

Figure 4.7: Combination of streamwise velocity and Reynolds stresses. Note that the failure is marked in red

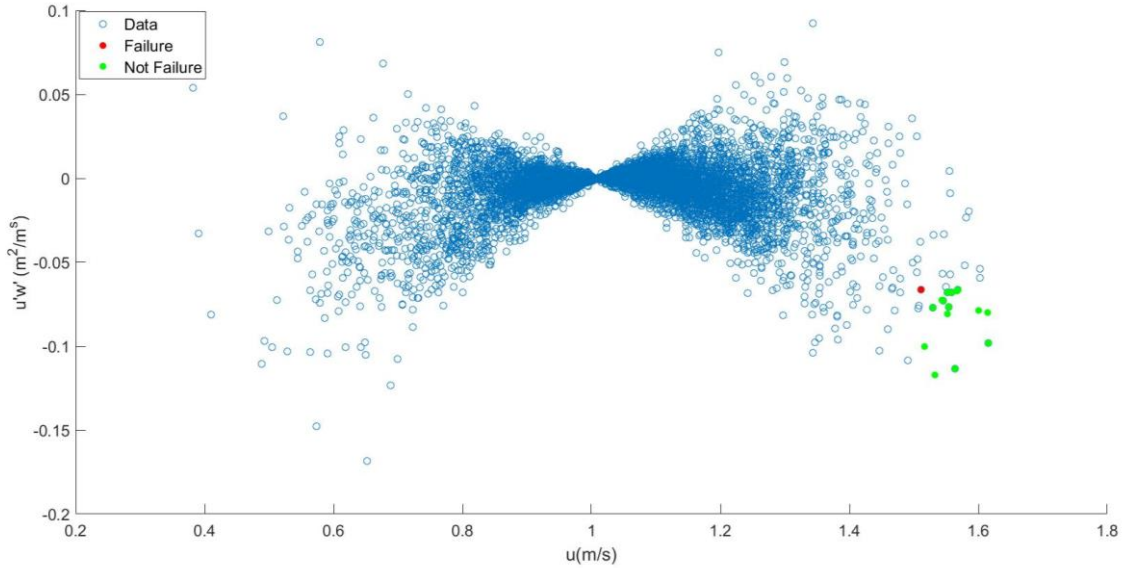

Figure 4.8: Combination of streamwise velocity and Reynolds stresses. Note that the failure episode is marked in red and the episodes with higher velocity and stress are marked in green

Figure 4.7 shows that the failure is associated to the episode with the highest combination of Reynolds stress and streamwise velocity. By contrast, Figure 4.8 shows that there are episodes with higher velocity peaks combined with higher stresses that do not lead to failure. This figure indicates that the combination of streamwise velocity and the shear stress cannot solely explain the initiation of motion of a block.

In line with this finding, Hofland (2005) concluded that a stone entrained during the presence of an increase in streamwise and downwards velocity (Q4) was often combined by an initial lift by an increase in vertical velocity (Q2). Hence, even that the sweep episodes were mostly present on failures, they do not completely govern the entrainment of a stone.

At the present study, the recorded data did not allow to conclude the combination of Q2 and Q4 events was the failure mechanism. Thus, there is a gap of knowledge in the explanation of the failure mechanism of block mattresses that was not possible to fill at the present study.

4.4 Weak point at the last row

The failure of the block mattress was placed at the last row of the block. To understand the reasons of the weakness, two different tests were done. In the first one, the flow over the last block was studied, by measuring a series of point around the last block.

Figure 4.9 shows the position of the measuring point and the value of the mean velocity at that position. By observing the values of the mean velocity, it can be concluded that the last block acts as a backward facing step (BFS). The flow over the block is accelerated and behind it, there is a recirculation area with negative mean velocities. Thus, instead of acting as a decelerating flow on an expansion, the velocity increases over the last block with Froude numbers close to 1.

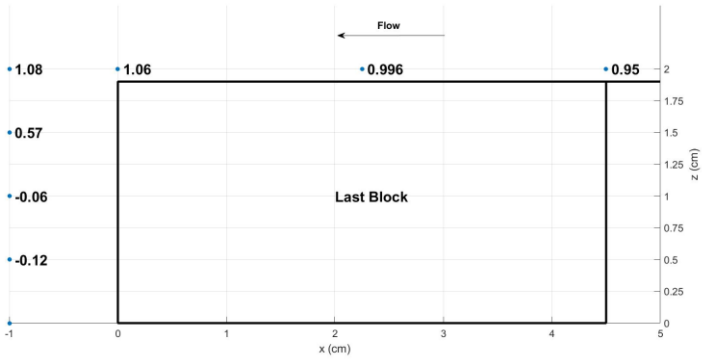

Figure 4.9: Mean velocity around the last block in various points. The values are placed at the measuring point and the units are (m/s)

This acceleration of streamwise velocity can be the cause of the weakness of the last row comparing to middle blocks of the mattress. Following this idea, a second series of test were done comparing the last block as an open edge (free downstream) with the last block as a close edge (transition with another mattress).

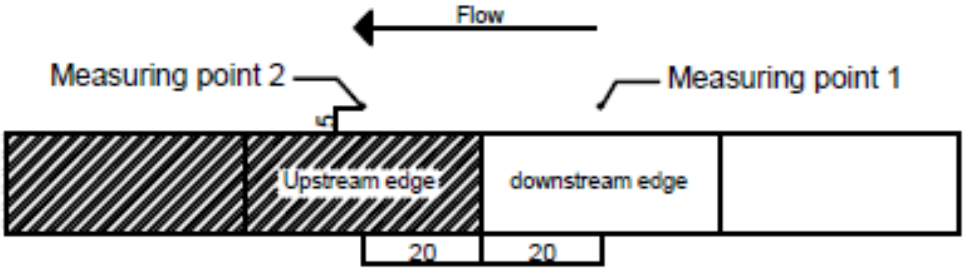

Figure 4.10: The measuring set-up to compare the flow parameters between an open edge (without the upstream edge of the second mattress) with a close edge (transition between mattresses). The distances are in mm. Note that there is not connection of geotextile between the mattresses.

Measurement	$\overline{u}$ [m/s]	Max u [m/s]	σ_u [m/s]	$\sqrt{k}$ [m/s]	h [cm]	Leddy [cm]
1 (Open)	0,98	1,42	0,124	0,115	3.5	2
1 (Close)	0,76	1,32	0,158	0,134	4	2,3
2 (Open)	1,09	1,61	0,115	0,108	3	2,2
2 (Close)	0,67	1,26	0,148	0,127	4	2

Table 4.4: Values of the flow properties comparing an open and close edge

Table 4.4 shows that in an open edge situation the streamwise velocities (mean and maximum values) are higher than in an close edge situation. By contrast, the turbulence intensity are higher in close edge situation. Hence, it seems that the turbulence is not the cause of the weakness.

Besides, figure 4.11 shows the autocorrelation function of the four measurements. Graphically seems that the eddy size at the close edge is slightly larger. However, the values on table 4.4 show that the eddy size is similar at the four points. The eddy size is limited by water depth.

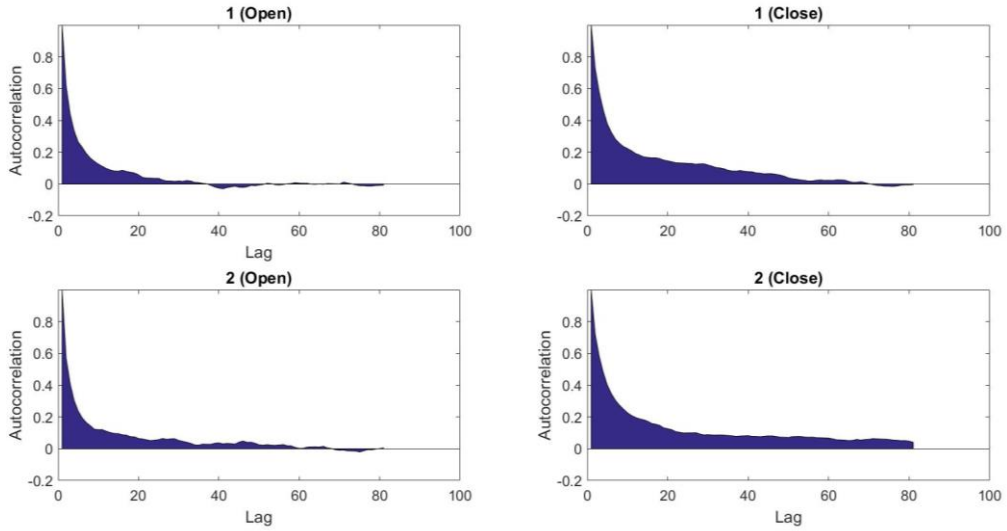

Figure 4.11: Autocorrelation function of the four measurement points to compare the flow over an open edge and a close edge

In addition to this experiment, some tests were done to study the failure of the close edge. However, failure discharge was above the limit of the safety of the flume. Thus, any failure of a close edge situation was recorded. However, it can be concluded that the close edge situation is more stable than the open edge situation. Van Velzen and De Jong (2015) concluded that the critical velocity in a close edge in more than twice bigger than the one for an open edge. This conclusion is aligned with the behaviour observed at the present study.

Besides, the displacement of the middle blocks was studied. Figure 4.12 shows that the blocks are kept in place by the presence of adjacent blocks in the middle blocks. Thus, the block rows provide to each other cohesion that limited the displacement. At middle block locations of the mattress, some blocks were displaced but the displacement was smaller than the failure threshold.

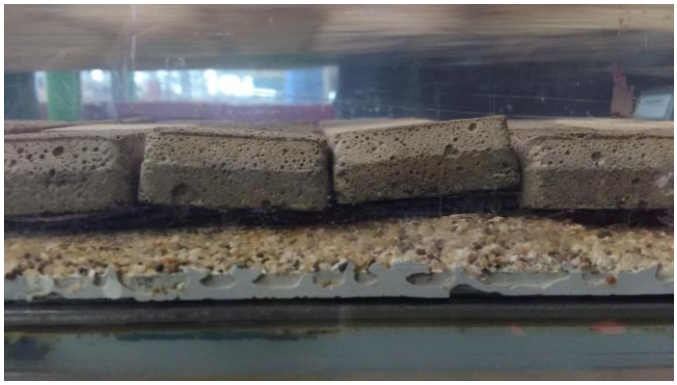

Figure 4.12: Displacement of the middle block limited by the cohesion supplied by the adjacent blocks. Unlike the edge situation, in the middle of the mattress, the blocks are surrounded by blocks downstream and upstream.

4.5 Conclusion and last row proposal

In this chapter, the flow structures associated to failure and the weakness of the last block were studied. The analysis of the failure mechanism was done by synchronizing the velocity time series with the displacement of the blocks. The failure signal shows that the displacement of the block is related to a peak of velocity in streamwise velocity. Additionally, this failure is preceded by an increase of the exposure area of the block at discharges much lower than the failure discharge.

However, the presence of higher peaks of higher streamwise velocity before the failure showed that the streamwise velocity cannot solely explain the initiation of motion. Besides, the combination of velocity and Reynolds stresses neither explain the failure mechanism. Therefore, further studies should be done to explain the failure mechanism of a block mattress.

Two series of test were done to study the weakness of the last row. The first one shown that the flow over last block of the mattress act as a backwards facing step, accelerating the streamwise velocity. The second test series, show that comparing an open edge and a close edge, the presence of another block downstream the edge increases the turbulent intensity but decreases the streamwise velocities. Besides, the observation of the middle

blocks of the mattress showed that the adjacent block add cohesion to the blocks. Therefore, the lack of blocks downstream the last block leads to facilitate the rotation of the block.

According to the findings describing above, a more stable shape of the last block should provide a smoother transition to avoid the acceleration of the flow. Also, it should provide and extra stability to balance the lack of cohesion of the adjacent blocks. However, this extra stability should not be go together with an increase of the exposure area. Figure 4.13 shows a proposed shape of the last row block with the same weight that should be studied under turbulent flow.

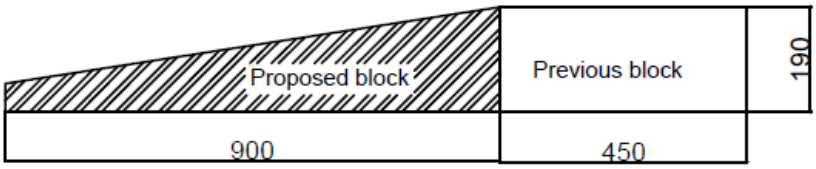

Figure 4.13: Sketch of the proposed last block shape to be checked in further researches. Note that the distances are in mm

Additionally, loose rock can be placed to avoid the behaviour of the last block as a BFS. In situations where there is not a limitation of space downstream of the block, a layer of rocks is usually placed. In this case, last block will not behave as a BFS but the variation of roughness induces an extra turbulence that can reduce the stability of the block. In these situations, the length of the mattress should be large enough to ensure that the flow at the downstream end is not able to induce any damage. Hence, the failures under different situations of the present one at this study (close edge and middle block failures) should be studied.

5. Stability equation

5.1 Introduction

After studying the flow structures related to failure, a new stability equation based on Pilarczyk equation was developed. For that propose, the previously analysed failures were associated to mean velocity and turbulence intensity values. The purpose of this chapter is to describe the failure velocity as an addition of mean velocity and turbulence intensity, multiplied by a magnification factor. The turbulence magnification factor (α) was derived by two different approaches, as a physical parameter and as a fitting parameter.

Besides, the stability parameter corresponding to an open edge of the block mattress was derived for the different approaches. Finally, the derived equation was compared to the equations available in literatures.

The structure of this chapter is as follows. Section 5.2 describes the development of the data base and the derived fitting equations. The values of α are studied in sections 5.3 and 5.4. Section 5.5 is focus on the stability parameter and the α derivation approaches are compared in section 5.6. In section 5.7 the new developed equation is compared with the original Pilarczyk equation and the modification proposed by the Rock Manual (2007) and finally, section 5.8 summarizes the obtained conclusions.

5.2 Database

The first step to derive a stability equation from the recorded failures was to develop a data base. As was mentioned in chapter 3, the data base was recorded for the four configurations of the test. The main objective of the data base was to relate a certain discharge with the associated flow parameters; mean velocity and turbulence intensity. Figure 5.1 shows graphically the fitting for the four data bases and derived equations from the data, which were used to define the flow parameters on the failures.

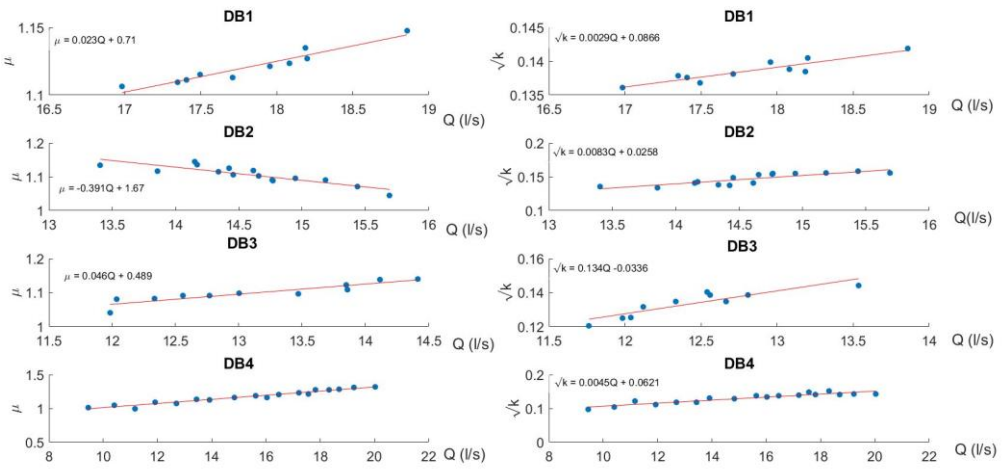

Figure 5.1: Summary of the results of the data base. The measured values are fitted by a linear approach. The derived equations are also present

Thereafter, the failure discharges were combined with the derived fitting equations. The fitting equations show that the mean velocity and the turbulence intensity increase with increasing discharge. However, in configuration 2, the mean velocity decreases with increasing discharges. Annex 6 studies a possible explanation for this behaviour. Based on these results, a mean velocity and a turbulent intensity were associated to each failure to derive a stability equation. Table 5.1 shows the computed values.

Failure	Qfail [l/s]	U_{peak} [m/s]	$\overline{u}$ [m/s]	$\sqrt{k}$ [m/s]	σ_u [m/s]
1	18,02	1,55	1,13	0,139	0,148
2	17,57	1,45	1,12	0,138	0,148
3	17,70	1,49	1,12	0,138	0,148
4	17,76	1,64	1,12	0,138	0,148
5	14,86	1,46	1,09	0,149	0,172
6	14,55	1,47	1,11	0,147	0,169
7	14,68	1,56	1,10	0,148	0,170
8	14,52	1,56	1,11	0,146	0,169
9	13,12	1,60	1,09	0,142	0,167
10	13,51	1,43	1,11	0,143	0,167
11	12,96	1,57	1,09	0,141	0,165
12	12,37	1,59	1,06	0,134	0,155
13	17,73	1,68	1,25	0,142	0,154
14	17,75	1,68	1,25	0,141	0,154
15	16,57	1,52	1,21	0,137	0,148
16	17,29	1,65	1,24	0,140	0,152

Table 5.1: Summary of flow parameters obtained by the combination of the failure discharges and the data bases

5.3 Alpha value based on peak velocity

Chapter 4 showed that failure of the block was related to a peak of streamwise velocity. Thus, the failure velocity of the block could be related to this peak of velocity [5.1]. To describe the peaks of velocity in non-uniform flow related to entrainment of stones, Jongeling et al. (2003) proposed an approach where the peaks were described as a combination of mean velocity and turbulence [5.2]. This structure was followed by other authors like Hofland (2005). In a comparable way, Hoan (2008) used the standard deviation in streamwise velocity as the quantification factor for turbulence intensity [5.3].

Following this structure, the value of the turbulence magnification factor were obtained by combining the recorded failures and the developed data base.

$$U_{fail} = U_{peak} \quad [5.1]$$

$$U_{peak} = \bar{u} + \alpha\sqrt{k} \quad [5.2]$$

$$U_{peak} = \bar{u} + \alpha\sigma_u \quad [5.3]$$

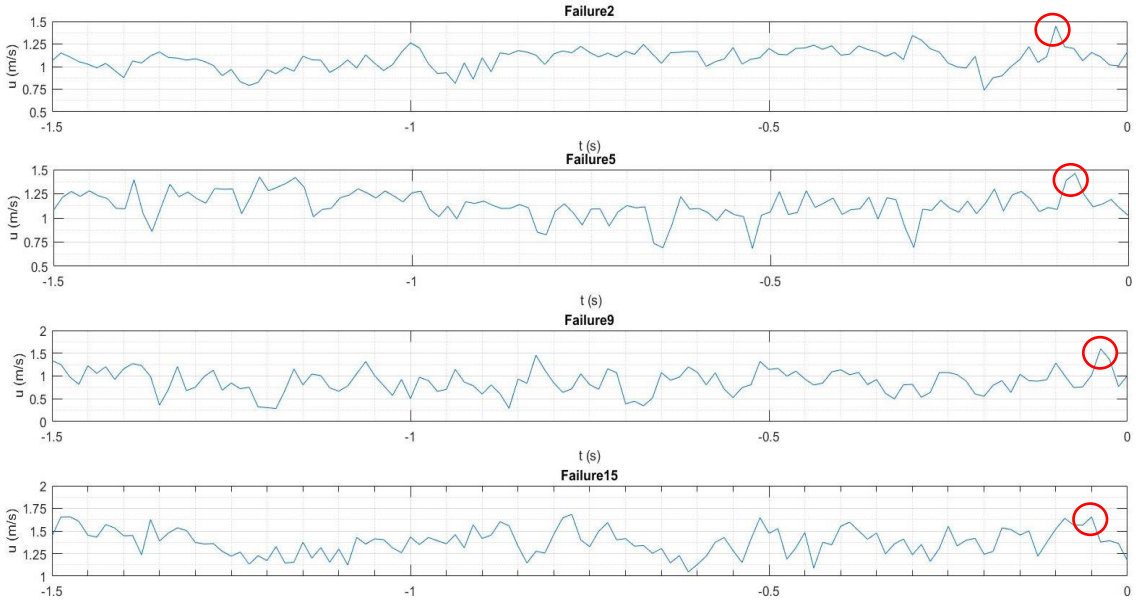

Figure 5.2: Signal of four different failures. In red circles, the peak of velocity considered as failure velocity.

Figure 5.2 shows the velocity signals close to failure of the mattress (t_0 is the synchronized failure time for all the failures). The highlighted peaks are the peaks related to failure episodes. These peaks were used to derived the value of the turbulence magnification factor (α) for the recorded failures [5.4] and [5.5]. The obtained values for α were computed using both total kinetic energy and standard deviation in streamwise velocity. Hoan (2008) concluded a value of α equal to 3 and 3.5 for Jongeling equation [2.17]. Figure 5.3 shows that the obtained values were aligned with this conclusion. Moreover, table 5.2 summarized the derived values.

$$\alpha_k = \frac{u_{peak} - \bar{u}}{\sqrt{k}} \quad [5.4]$$

$$\alpha_\sigma = \frac{u_{peak} - \bar{u}}{\sigma_u} \quad [5.5]$$

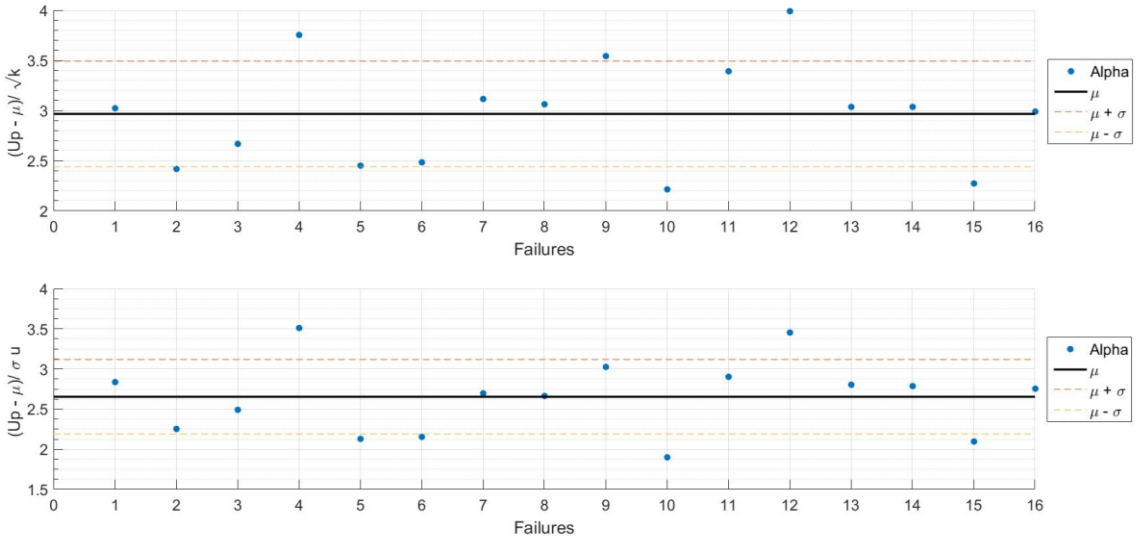

Figure 5.3: Alpha values derived based on peak velocities of the failures. The turbulent intensity is computed for both kinetic energy and deviation in u

	$\sqrt{k}$	σ_u
$\bar{\alpha}$	2,92	2,62
σ_α	0,58	0,51

Table 5.2: Summary of the results derived for alpha values based on peaks of velocity leading to failure

According to the conclusion obtained in chapter 4, this failure peaks do not represent the maximum velocity of the signal. Episodes of higher velocities were recorded in most of the signal (Figure 4.8). Thus, the derived parameter describes a safety threshold of stability. This implies that the peaks can be interpreted as the minimum velocity that can induce failure.

5.4 Alpha values as a fitting parameter

In the previous approach, α was related to a physical parameter of the flow. However, previous authors (Jongeling et al (2003), Hofland (2005) and Hoan (2008)) considered α as a fitting parameter. The value of α, thus, was based on the best data collapse. The proposed stability equation was based on Pilarczyk stability equation [2.12]. For the same block thickness, the failure velocity could be expected to be the same [5.6]. Figure 5.4 shows the standard deviation of the failure velocity for different values of α.

$$U_{fail} = \bar{u} + \alpha\sqrt{k} \qquad [5.6]$$

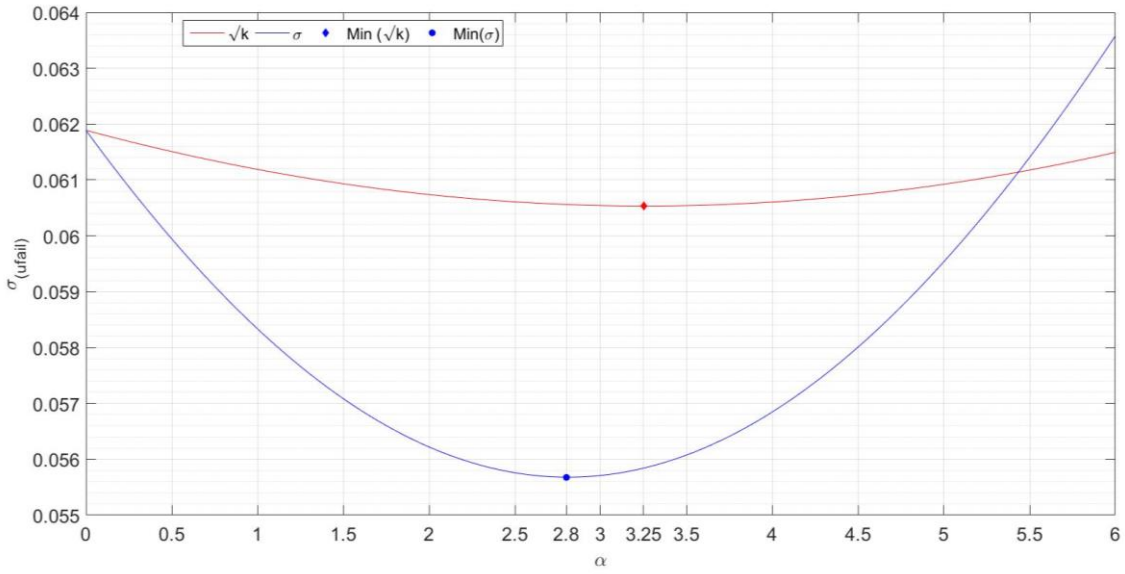

Figure 5.4: Values of the standard deviation of the failure velocity for the measured failures for different values of alpha values

In line with the results obtained in the previous approach, the best collapse of the failure velocity was around α values of three.

	$\sqrt{k}$	σ_u
$\bar{\alpha}$	3,25	2,8
$\sigma_{u_{fail}}$	0,06	0,056

Table 5.3: Summary of the derived values for alpha as a fitting parameter.

Table 5.3 shows the summary of the obtained results. Results show that the deviation of failure velocity was small for any value of α. However, figure 5.4 shows that there was an optimum point for α values around three, even that the differences were small. This value is expected to be consistent if a larger amount of failures are considered.

5.5 Stability parameter

In previous sections, the value of the turbulence magnification factor α has been discussed. Thereafter, the different parameters of the Pilarczyk equation will be studied, with special attention to the stability parameter.

$$\Delta D = 0.035 \frac{\Phi}{\Psi} \frac{K_h}{K_s} \frac{(\bar{u} + \alpha TI)^2}{2g} \quad [5.7]$$

Where:

$\Delta = Relative\ density\ (-)$

$D = Characteristic\ dimension/thickness\ \ (m)$

$g = Acceleration\ of\ gravity = 9.81\ {}^{m}/_{s^2}$

$\bar{u} = Averaged\ flow\ velocity\ ({}^{m}/_{s})$

$\Phi = Stability\ parameter\ (-)$

$\Psi = Critical\ Shield\ parameter\ (-)$

$\mathrm{TI} = Turbulence\ intensity\ ({}^{m}/_{s})$

$K_h = Depth\ parameter\ (-)$

$K_s = Slope\ parameter\ (-)$

Equation 5.7 shows the proposed modification for Pilarczyk equation. Based on the known parameters and the obtained results, the stability parameter can be derived. Table 5.4 summarizes the known parameters.

Parameter	Value	Explanation
Δ	1.31	Provided by the supplier
$\boldsymbol{D}$	0.019	Thickness of the testes blocks
$\boldsymbol{\Psi}$	0.07	Value for block mattresses
$\boldsymbol{K_h}$	1	Measurements close to the bottom (5mm)
$\boldsymbol{K_s}$	1	No slope

Table 5.4: Summary of the known parameters of the proposed stability equation

Thus, with the known parameters and the computed parameters of the failures, the stability parameter [5.8] was studied based on the four obtained values of α at previous sections. In the following sections, the notation *peak* will be related to the approach described in section 5.3, based in peaks of velocities. Besides, the notation *op* will be related to the approach described in section 5.4 where the value of α was derived based on an optimization process.

$$\Phi = \frac{\psi}{0{,}035} \frac{2g\Delta D}{(\bar{u}+\alpha\sigma_u)^2} \qquad [5.8]$$

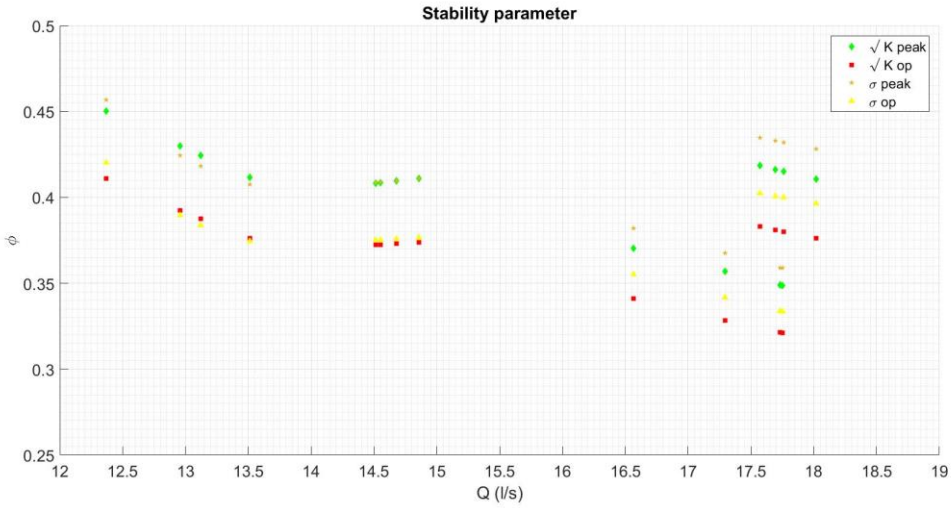

Figure 5.5: Stability parameter for the recorded failures for the four derived α values. Note that the notation peak refers to the first approach, while notation op refers to the second approach.

Figure 5.5 shows graphically the derived stability parameter for the recorded failures. The graph shows that the values were spread around 0.4. Moreover, table 5.5 summarizes the derived values for the stability parameter. The results provided as a mean value and a standard deviation are a useful tool for probabilistic design approach. Additionally, the maximum and minimum values specify the range of the results.

	α	$\bar{\Phi}$	σ_Φ	**Max Φ**	**Min Φ**
$\alpha_{\sqrt{k}\,peak}$	3	0,400	0,031	0,450	0,349
$\alpha_{\sqrt{k}\,op}$	3,5	0,366	0,027	0,411	0,321
$\alpha_{\sigma_u\,peak}$	2,6	0,407	0,029	0,456	0,359
$\alpha_{\sigma_u\,op}$	3	0,376	0,026	0,420	0,334

Table 5.5: Summary of the obtained results for the stability parameter for the four developed approaches

5.6 Comparison between approaches and selection of alpha

In previous sections, two different approaches were defined for the derivation of the turbulence magnification factor. As could be expected, the values of the stability parameters are bigger for the first approach, based on peaks of velocities than for the second one. This matches with the meaning of both approaches.

The first approach can be described as the minimum streamwise velocity that leads to failure, as mentioned in section 5.3. Thus, the definition of α relies on the idea that there

is a threshold of motion based on streamwise velocity. Even that conclusions in chapter 4 showed that the motion of the block cannot be solely associated to streamwise velocity, in case of using it as a design formula, it can be considered as a safe approach. Thus, it can be defined as a conservative design.

By contrast, in the second approach, α cannot be related to any physical meaning and it acts as a fitting parameter. Previous authors (Jongeling (2003), Hofland (2005) and Hoan (2008) also derived α in the same way. Therefore, it is a more accurate approach and it does not imply any assumption. Besides, it does not consider any safety factor. This give more tools for the designer, as the safety coefficient can be decided based on the risk of different situations and the accuracy of the flow information. In addition, the use of certain safety factor can be different for a probabilistic or a deterministic design.

Based on the previous conclusions and on the obtained results in table 5.5, the use of standard deviation in *u* as the turbulence intensity and a turbulence magnification factor α = 3 was the most suitable combination for the available data. Thus, equation [5.7] was compared to the previously available equations in the following section. As the comparison was based in a deterministic approach, the maximum value of the stability parameter Φ = 0.42 should be used.

5.7 Comparison of stability equations

In previous sections, the development of a stability equation based on Pilarczyk equation was studied. Thereafter, in this section, the new stability equation was compared to previous equation.

$$\Delta D = 0.035 \frac{\Phi}{\Psi} \frac{K_h K_t^2}{K_s} \frac{(\bar{u})^2}{2g} \qquad [5.9]$$

Pilarczyk original equation [5.9] includes turbulence intensity as a multiplication factor K_t^2 that takes its value based on some guide values. According to Pilarczyk (2001) for the tested situation a value of K_t^2 between 1.5 (increased turbulence) and 2 (Heavy turbulence) should be taken. Thus, the turbulence factor is rough and unprecise.

However, Rock Manual (2007) provided an expression based on relative turbulence intensity to compute the value of K_t^2 as a turbulence magnification factor.

$$K_T{}^2 = \frac{1+3r}{1.3} \qquad [5.10]$$

To compare the new proposal with the equations available in literature, the required block thickness for the recorded failures was computed. According to Pilarczyk (2001), for edge of the mattresses a stability parameter equal to 1 should be used. Table 5.6 summarizes the parameters used in the comparison. The values for the complementary parameters are the same of table 5.4.

Parameter	Original	Rock Manual	New proposal
Φ	1	1	0.42
Turbulence intensity	$K_t^2 = 1.5$	$K_t^2 = \frac{1+3r}{1.3}$	$\alpha = 3$

Table 5.6: Summary of the parameters used at the comparison additional to table 6.4

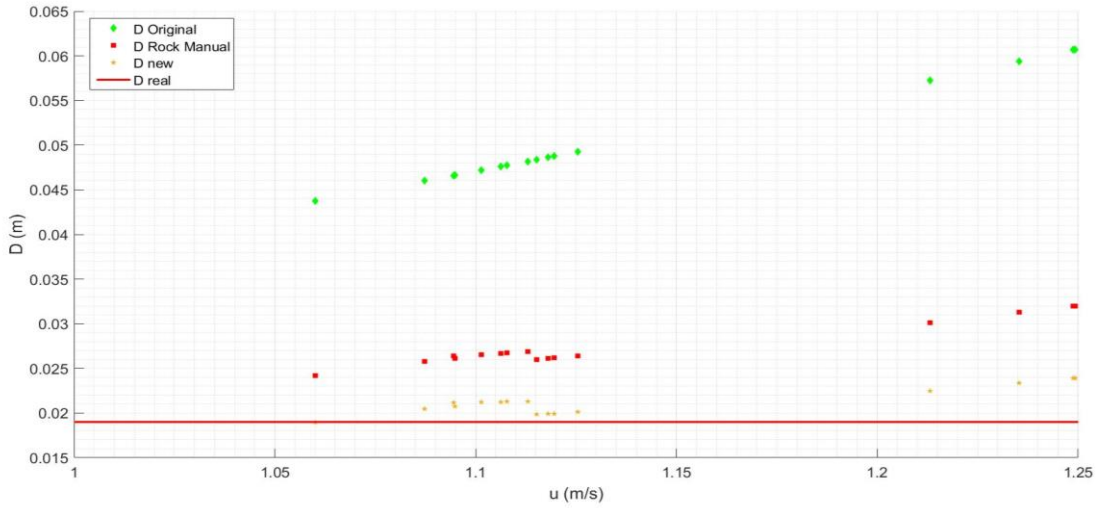

Figure 5.6: The computed block thickness for the recorded 16 failures by the 3 studied approaches and the real thickness

Figure 5.6 shows that the three approaches over dimension the block thickness. However, the innovative approach shows the best collapse to the real thickness. Figure 5.7 and 5.8 show the relative error of the three equations for each failure and the mean value.

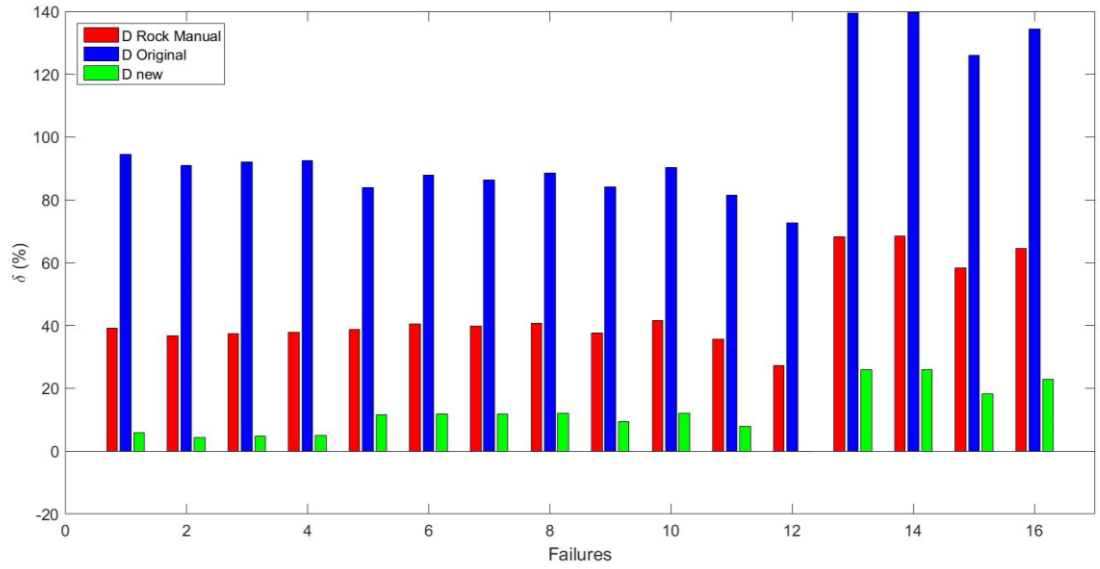

Figure 5.7: Relative errors of the calculated block thickness for each of the recorded failures

Figure 5.8 shows that the new proposed stability equation is more accurate than the equations available on literature. Comparing to first equation, Pilarczyk equation with the turbulence magnification factor K_t^2 based on relative turbulence intensity, there is an increase of accuracy without requiring any extra information. Equation 5.11 shows that the new proposed equation can also be computed based on relative turbulence intensity.

$$\Delta D = 0.035 \frac{\Phi}{\Psi} \frac{K_h}{K_s} \frac{\left(\bar{u}(1+\alpha r_u)\right)^2}{2g} \qquad [5.11]$$

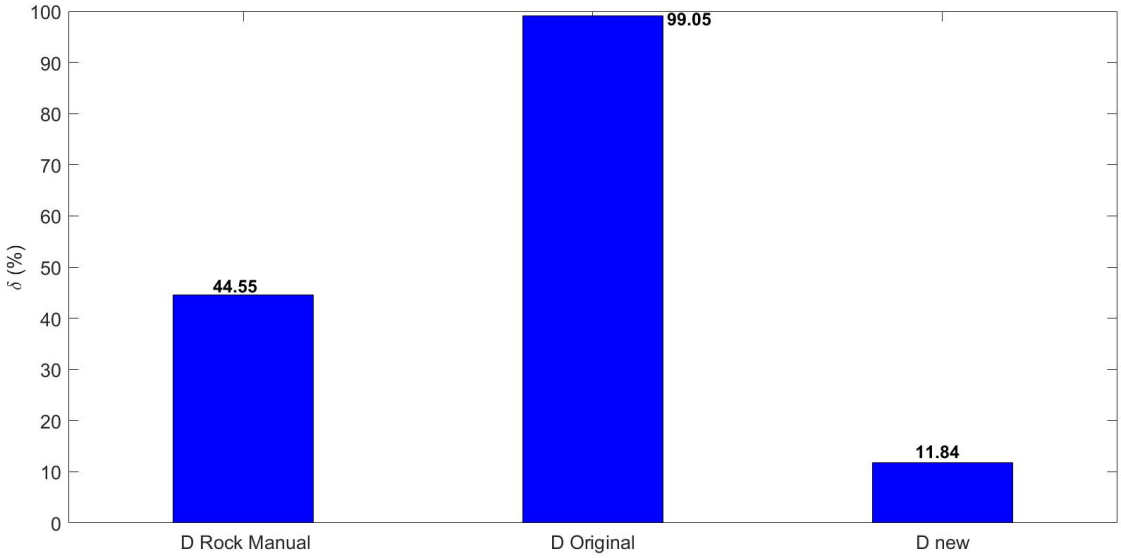

Figure 5.8: Mean value of the relative errors of the calculated block thickness for the recorded failures

5.8 Conclusions

In this chapter, the development of a new stability equation for block mattresses based on Pilarczyk equation has been studied. In the new equation, turbulence intensity is included in a quantitative way and based in a measurable statistical magnitude (relative turbulence intensity). Instead of adding the turbulence as a multiplication factor, the turbulence intensity is added to the mean velocity following the structure of the lasts publications in stability.

$$U_{fail} = \bar{u} + \alpha \sigma_u \qquad [5.12]$$

The value of the turbulence magnification factor (α) was derived by two different approaches; based on the peak velocity leading to failure and based on the best fitting of the data. In both approaches the values of α was around 3, in line with the expected value based on previous literature. This confirms that the structure quantifying turbulence as an addition to the mean velocity developed for loose rock is also applicable for block mattresses.

Besides, the stability parameter for the new developed equations has been derived. Although the short amount of failures recorded (16), the results show consistency around 0.4.

Finally, Pilarczyk equation and the new proposed equation have been compared. Additionally, the turbulence multiplication factor proposed by the Rock Manual (2007) [5.13] has been also compared. The new equation has shown more accurate results than both Pilarczyk equations without requiring any extra information.

$$K_T{}^2 = \frac{1+3r}{1.3} \qquad [5.13]$$

The comparison between the equations showed that the new developed equation provides a more accurate design that implies a saving in the block thickness. Moreover, the stability parameter was defined as a mean value, a standard deviation and minimum and maximum values. This information is a useful tool for probabilistic design or to select the safety factor based on the designer criteria and the risk values.

6. Discussion

6.1 Introduction

At previous chapters, the experimental arrangement, the failure mechanism and the stability of the block mattress were studied. The results and conclusions previously obtained are discussed at the present chapter and the uncertainties underlying the experiments and the reliability of the results are debated. Moreover, an analysis of the flow is done to check the turbulent behaviour and to verify the consistency of the measurements.

6.2 Experimental arrangement

In the third chapter, the experimental configuration was checked. One of the critical issues during the tests was to ensure the 2-D behaviour of the flow. To guarantee this, the connections of the edges of apron to the flume were sealed with silicone. Moreover, a wooden piece was placed at the downstream end of the apron to avoid the impact of the flow to the front row of the mattress. When the flow under the apron was not stopped, the failure of the block mattress was placed at the first row, inducing scale effects. After taken all the measures to stop the flow, it was concluded that there were not infiltrations that could disturb the two-dimensionality of the flow.

Figure 6.1: Details of the interface apron-mattress

However, the condition for the flow over the mattress was different. The width of the block mattress was smaller than the width of the flume. Thus, at both sides of the mattress

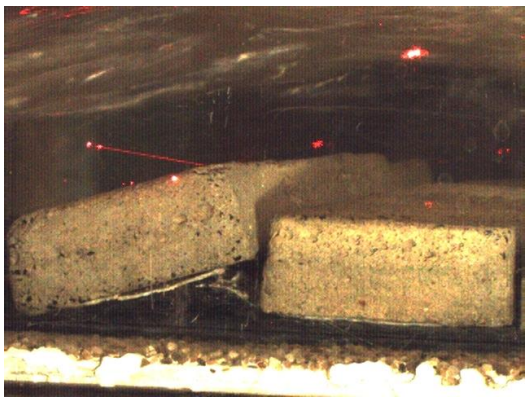

Figure 6.2: Failure of the last row of the mattress

there was a region of the flume without mattress that could modify the flow. The measuring point of the LDV was placed at the middle of the block and the failure was associated to the lifting of the whole last row of blocks (Figure 6.2).

However, in failure 14 the signal was interrupted by the lifting of only an edge block. The failure of the rest of the blocks of the row was at similar discharge but without the possibility of measuring the signal. This, should not have a significant effect on the development of the conclusions since the failure discharge is not altered.

In conclusion, the flow over the flume can be considered as two-dimensional and there are not significant scale effects that can disturb the results. However, it is recommended that in further studies the block mattress width should be the same of the flume width.

6.3 Flow analysis

Quadrant analysis

Raupach, in 1981, (Thompson 2017) performed a quadrant analysis that relates the velocity fluctuations to flow events. Based on the sign of the vertical and streamwise velocity fluctuation, four different events could be defined. He concluded that the events in which u' > 0 and w' < 0 (sweep) are the most important contribution to the Reynolds stress near the bed and hence, to instability. The failure analysis conclusions were in line with this assumption, as the failures were related to sweep episodes.

Besides, according to Thompson (2017), in a turbulent flow the combination of a negative vertical velocity with a positive streamwise velocity a vice versa are more likely to occur than both positive and negative. A quadrant analysis was done for four random tests, one for each configuration, to verify the frequency of each episode on the measured velocity signals.

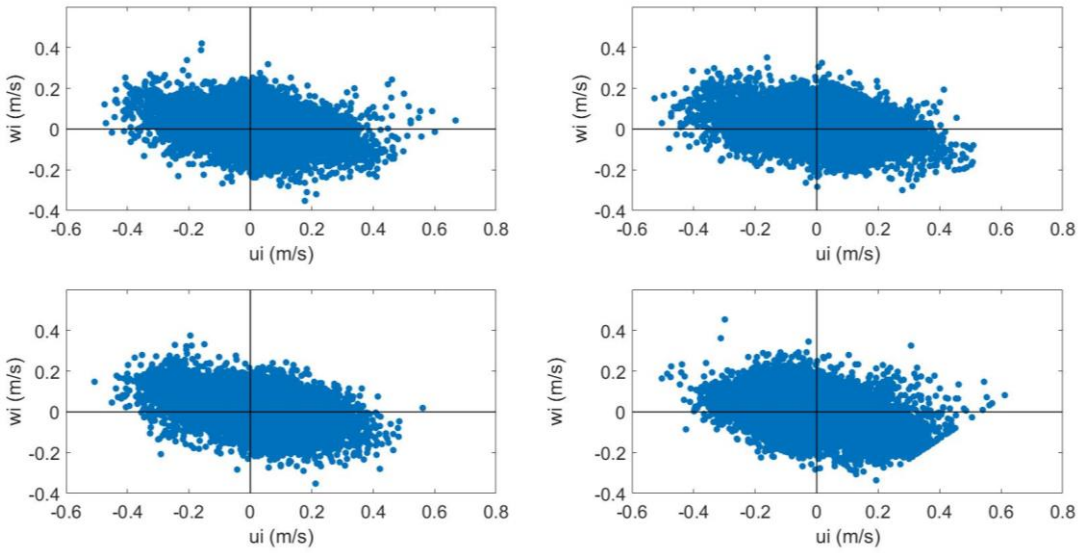

Figure 6.3: Combination of velocity fluctuation between streamwise and vertical velocities. Four random samples are represented, one of each configuration.

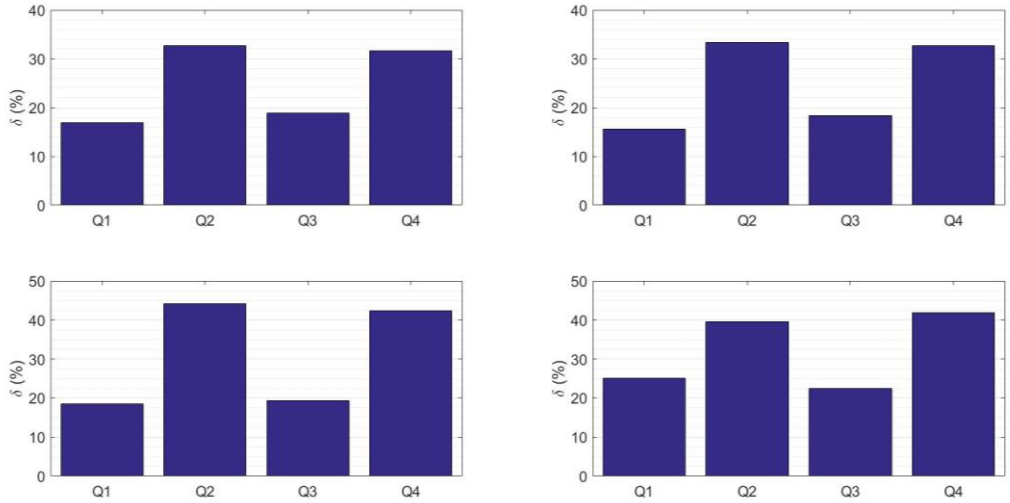

Figure 6.4: Percentage of occurrence of the different quadrants for four random series, one for each configuration

Figure 6.3 and 6.4 show that the combinations of positive shear stress (Q2 and Q4) were more likely to occur at the measured flow. This result conclude that the measured signals behaved according to the expected patterns.

By contrast, the flow episodes related to the increasing of exposure of the block could not be defined. According to Hofland (2005) this lifting can be related to ejections episodes (Q2). The measurement accuracy of the displacement with the camera did not allow to relate this displacements to the velocity signal. In further studies, the possibility of using whole profile measurement devices like PIV or to install accelerometers inside the blocks should be studied.

Probabilistic distribution of the velocity signal

According to Uijttewaal (2017), for ideal homogeneous and isotropic turbulence, the velocity fluctuations are distributed normally. To check the normality of the data, one sample of each configuration was analysed.

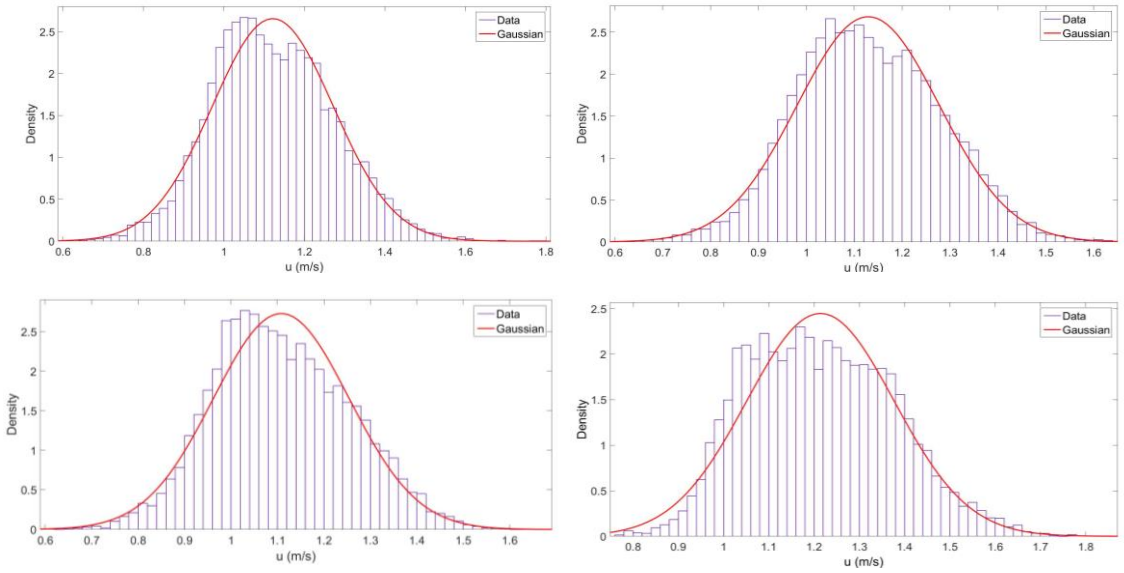

Figure 6.5: Comparison of 4 recorded data to a gaussian distribution. The data are the same signals used in quadrant analysis

Figure 6.5 shows that graphically the velocity signal fits well with a gaussian distribution. However, they show some asymmetry and a lack of data close to the mean. To analyse their properties, the skewness [6.1] and the kurtosis [6.2] of the signal were checked. In a normal distribution, the skewness has a value of 0 and kurtosis three.

$$S = \frac{\mu_3}{\sigma^3} = \frac{\overline{(u-\bar{u})^3}}{\sigma^3} \qquad [6.1]$$

$$k = \frac{\mu_4}{\sigma^4} = \frac{\overline{(u-\bar{u})^4}}{\sigma^4} \qquad [6.2]$$

Data base	Skewness	Kurtosis
1	0.179	2.21
2	0.087	2.67
3	0.205	2.77
4	0.255	2.62

Table 6.1: Values for the skewness and flatness of four samples of data, one for each configuration

Four cases showed similar values that match with the graphical observation. A positive skewness is related to an asymmetry to the right, as figure 6.5 shows. This asymmetry implies that there are more values lower than mean. A kurtosis lower than 3 implies a platykurtic distribution, which implies that there is a lack of values close to the mean value.

Summarizing, the study of the normality of the data shows that the streamwise velocity fluctuations have some deviation from a gaussian distribution, although these deviations are not very large. According to Bulmer (1979) if the deviation is lower than 0.5, the distribution can be considered as gaussian. At the studied data, only the kurtosis from the data base 1 has a larger deviation than the limit.

In chapter 5, the turbulence magnification factor (α) value was defined as three. In a gaussian distribution, 99.87% of the data is lower than the mean plus three times the standard deviation. The distribution of the fluctuations shows good fitting to a gaussian distribution that justifies the value of α as three. However, the values of skewness and kurtosis show that some deviation from this value is feasible.

6.4 Failure mechanism

In chapter 4, the failure mechanism of the block mattress was studied. An episode of increasing shear stress, due to a peak of streamwise velocity combined with downwards vertical velocities (sweep) was related to the failure. However, after analysing the highest episodes of combined streamwise velocities and Reynolds stresses, the results show that

higher values not leading to failure were present before the actual failure. Thus, the peaks of velocity cannot solely explain the failure of the block. The obtained data was not enough to determine completely the failure mechanism.

There are some reasons that can explain the lack of this data. The measurements were obtained by a single point measurement device (LDV). The intensity and the duration of the different episode cannot be defined by these devices. The size of the passing eddies can play a key role on the initiation of motion (Hofland 2005). Thus, a whole field measurement device (PIV) can be used in further researches to study the size and intensity of the eddies.

Moreover, the measuring frequency of the camera was 20 Hz and the LDV was 80 Hz. It is feasible that the measuring frequency was too low to characterize accurately small-scale episodes that can be related to failure. Additionally, the difference of measuring frequency between the devices could lead to loose some relevant information. For this reason, a different device should be used in further studies to analyse the failure mechanism.

An accelerometer can be added to the block to record the displacements with higher sample rate, synchronized with the velocity measuring device. At the present study, the possibility of using an accelerometer was considered. However, the size of the block did not allow to add it without disturbing the block-flow interaction. If an accelerometer is attached to the block, special attention should be taken to guarantee that the influence on the weight of the block and on the exposed area is minimum.

6.5 Alpha value and stability parameter

Alpha value

In chapter 5, the turbulence magnification factor α and the stability parameter were studied. α value was derived by two different approaches and in both of them, the derive values were close to three. The analysis of the data was done for four configurations where the range of flow behaviour was narrow. This can lead to certain uncertainty on the derivation of the value and its consistency for a wider range of flows. However, this value is in line with the proposed value of α by previous author on the development of stability equation for loose rocks. Therefore, it can be expected that the derived α will maintain similar values for further studies with different flow behaviours.

Stability parameter

The stability parameter was derived in chapter five based on the recorded failures. The obtained values provided an accurate design tool. Though, the parameter was derived using a single block thickness. In further studies, the consistency of the derived value should be tested for different thicknesses. Moreover, the available combination of block thickness and flume capacity only allowed to check the stability of an open edge at the end of the mattress. In further studies, the stability of close edge (transition) and middle blocks should be tested.

However, even that some research will be still needed, the results obtained in this study can be consider of important utility. The developed new equation makes the first step for

including turbulence intensity in a quantitative way, providing an accurate tool for the design of block mattresses.

6.6 Comparison with previous studies

The present study can be considered as a continuation of the previous researches done by Van Velzen and De Jong (2015) and Smyrnis (2017). Therefore, in this section the obtained results will be compared and discussed with the results and conclusion of the previous authors.

Van Velzen and De Jong

The study carried by Van Velzen and De Jong was based on checking the stability of the block mattress under propeller induced loads. Thus, there were significant differences on the analyzed flow with the present study. However, some similarities on the derived results were present. The main conclusion of the study was the difference of stability between the open edge and the close edges of the mattress. According to the results, the critical velocity for close edge was more than double than for open edges. At the present study, the difference of stability between both edges with checked. However, the limitation of capability of the flume did not allow to quantify the difference on the critical flow.

By contrast, Van Velzen and De Jong described the failure process of the mattress as snow-ball effect. The uplifting of the edge block was eventually followed by the flip over of the mattress. At the present study, the edge uplifting was not followed by the removal of the mattress. The difference on the failure process can be related to the shielded position of the first row at the present study. The tests showed that the mattress was washed way when the flow impact on the first row was not stopped, both for infiltrate flow under the apron and for exposure of the front blocks.

Smyrnis

The study done by Smyrnis (2017) concluded that Pilarczyk equations under estimate the strength of the edge blocks. In line with this conclusion, the present study showed that the required block thickness for open edges was over dimensioned by Pilarczyk equation. Moreover, the present study confirms the key role of turbulence on the instability of the block proposed by Smyrnis.

Besides, Smyrnis (2017) defined a threshold of motion based on the combination of relative turbulence intensity and mean velocity. Figure 6.6 shows the same analysis done for the present study.

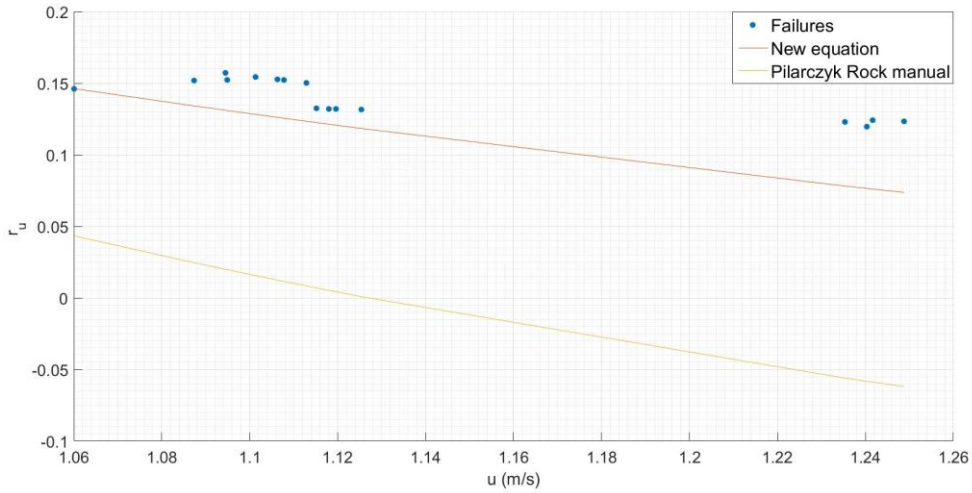

Figure 6.6: Mean velocity and turbulent relative intensity for the recorded failures. The lines represent the threshold for both new equation and Pilarczyk equation with the Rock manual turbulence coefficient

Figure 6.6 shows that the recorded failures follow a trend where for higher turbulent intensities the mean velocity at failure is smaller. The spread of results can be because of the stochastic nature of initiation of motion. Moreover, the two thresholds derived, new equation and Rock Manual variation show the higher accuracy of the developed equation.

In line with Van Velzen and De Jong, Smyrnis also recorded failures where the block mattress was washed away. At the recorded failures by Smyrnis that led to the total removal of the mattress and the washed away, the first row of the mattress was exposed to the flow. Thus, the differences of failure process can be explained by this fact.

7. Conclusions and design guideline

7.1 Introduction

In this chapter, the conclusions and the recommendations based on the developed research are given. According to the objectives described in section 1.2, the conclusions and recommendations are described based on the corresponding research question.

Moreover, this chapter also contains a design guideline where the relevant information for the design of block mattresses. The objective of this guideline is to provide an engineering tool to optimize the selection of the required block thickness.

7.2 Conclusions

I. Detailed knowledge of how the combination of mean flow and turbulence fluctuations induce failure of the block mattress:

- The turbulence fluctuations have a key role on the stability of the block. An episode of peak streamwise velocity is related to the failure of the mattress (section 4.3).
- An increase of the exposure area of the block is found before the failure of the block (Figure 4.9).
- The increase of streamwise velocity on failure is combined with a negative vertical velocity leading to a peak of increasing shear stress in a sweep episode (Figure 4.14).
- The streamwise velocity and the shear stress cannot solely explain the failure mechanism. However, the used measuring devices did not allow to completely describe the failure mechanism (Figure 4.16).
- The failure of the block mattress was found at the last row of blocks. Unlike the previous studies, the failure of the block did not imply the total removal of the mattress. The front row of the mattress in previous studies was not shielded by the apron. An exposed first row is related to the total removal of the block in failure, as was observed in Smyrnis (2017) (Section 3.2 and 4.4).
- In case of increasing the weight of the edge block mattress, this increase should never go related to an increase of the exposed area (section 4.3).
- The last row blocks behave as a backwards facing step, leading to an acceleration of the flow. The adjacent blocks provide cohesion that restricts the displacement of the block (Section 4.4).
- The close edge of a block mattress (transition point) is more stable than the open edge. The failure of the close edge was not possible to measure due to the capacity of the flume (Section 4.4).

II. Derivation of a block mattress stability equations that includes the turbulence intensity in a quantitative way.

- A new stability equation was proposed quantifying the turbulence intensity. The turbulence was included following the structure proposed for the stability of loose rock ($\bar{u} + \alpha\,\sigma_u$). The turbulence parameter is based in measurable statistical magnitude, the standard deviation in streamwise velocity (Section 5.5).
- The turbulence magnification factor (α) was derived for two different approaches. For both of them the derived value was close to 3 (Section 5.3 and 54).
- The value of α is in line with the values previously obtained by other authors for loose rocks. Thus, even than only a narrow range of different flows were testes it is expected that the value will mantain smiliar for if wider flow ranges are tested (Section 5.6).
- The new proposed stability equation describes more accuratelly the required block thickness than the previously available equations. This, provide an accurate tools to optimize the design of block mattresses (Section 5.7).
- The stability parameter for open edges was derived as a value of 0.4. Besides, the stability parameter is defined as a mean value, a standard deviation and maximum and minimum values (Section 5.5).

III. The derivation of a relation between the characteristic of the structure (weir height and apron length) to the flow parameters.

- A data base was developed for the four different configurations. From the data base, the value for the mean velocity and the turbulence intensity was derived based on the measured discharge (Figure 5.1).
- In three of the developed data based, both mean velocity and turbulence intensity increased for the increasing of discharge. In configuration 2 (h = 18.5 cm and d = 3h) the mean velocity decreases for increasing discharge (Section 5.2).
- The data base shows that the mean velocity and the turbulence intensity can be related to the characteristics of the structure and the discharge. The derived data base results are model results that do not represent any prototype scaling (Section 5.2).

7.3 Recommendations

I. Detailed knowledge of how the combination of mean flow and turbulence fluctuations induce failure of the block mattress:

- Particle Image Velocimeter (PIV) should be used to completely describe the failure mechanism. This device, used by Hofland (2005) will provide information about the size and the intensity of eddies related to failure mechanism.

- Accelerometers can be used, as an alternative to PIV, to measure the displacement of the block. This device will not measure the eddy size, but combined with the LDV, it will provide more accurate measurements with a higher measuring frequency that the high-speed camera used at the present study. The accelerometer added to the block should not increase the exposed area of the block.

II. Derivation of a block mattress stability equations that includes the turbulence intensity in a quantitative way.

- The value of the turbulence magnification factor (α) should be checked for a broader range of flows downstream of different structures. However, this value showed consistency with previous authors, so the value is not expected to vary.
- The stability parameter should be checked for different block thickness. The derivation of a stability parameter for a design equation should be based in tests for more than one thickness.
- A stability parameter for closed edged and middle blocks should be derived. The use of a larger flume or smaller block thickness will allow to derive the stability parameter for different configurations.

III. The derivation of a relation between the characteristic of the structure (weir height and apron length) to the flow parameters.

- More configurations should be tested in order to describe a broader flow and structure interactions. This will allow to describe a more accurate and handy design guideline.
- The optimum apron lenght should be studied. Results show that the required mattress thickness is reduced for longer aprons. An optimum position that reduces the required thicknes for the minimum apron length could reduce the costs.
- The behaviour of the mean velocity for configuration 2 (h = 18.5cm and d = 3h) should be studied to understand the effect of the apron length on the flow development and its influence on the mean velocity.

7.4 Design guideline

All the relevant knowledge regarding the design of block mattresses concluded during this study are summarized in a design guideline. The purpose of this guideline is to provide useful engineering knowledge for the design and optimize the thickness of the block mattresses.

New stability equation

$$\Delta D = 0.035 \frac{\Phi}{\Psi} \frac{K_h}{K_s} \frac{\left(\bar{u}(1+\alpha r_u)\right)^2}{2g}$$

Where:

$\Delta = Relative\ density\ (-)$

$D = Characteristic\ dimension/thickness\ \ (m)$

$g = Acceleration\ of\ gravity = 9.81\ {}^{m}/_{s^2}$

$\bar{u} = Mean\ velocity - averaged\ flow\ velocity\ ({}^{m}/_{s})$

$\Phi = Stability\ parameter\ (-)$

$\Psi = Critical\ Shield\ parameter = 0.07$

$r_u = Relative\ turbulence\ intensity\ in\ streamwise\ direction\ ({}^{m}/_{s})$

$\alpha = Turbulence\ magnification\ factor = 3$

$K_h = Depth\ parameter\ (-)$

$K_s = Slope\ parameter\ (-)$

Mean velocity and turbulence intensity

The following table described the mean velocity and relative turbulent intensity for the studied four configurations for a range of discharges extrapolated from the derived data base. The measurements were obtained close to the bottom and hence, the depth parameter should be considered equal to one. At the end of the section a small discussion about the depth parameter is included.

The proposed values of velocity and discharge have their corresponding units. Equations 7.2 and 7.3 proposed the values for non-dimensional values. At the present study, the accuracy of the water depth is limited and the values are kept dimensional. However, for further studies, the values non-dimensional values should be studied.

$$\bar{u}^{+} = \frac{\bar{u}}{\sqrt{gh}} \qquad [7.2]$$

$$Q^{+} = \frac{Q}{bh\sqrt{gh}} \qquad [7.3]$$

Where:

$h = Water\ depth \qquad (m)$

$b = Flume\ width \qquad (m)$

$\bar{u} = Mean\ velocity \qquad (m)$

$Q = Discharge \qquad \left({}^{l}/_{s}\right)$

Height	15cm				18.5 cm			
Apron length	3h		4h		3h		4h	
Parameter / Discharge (l/s)	$\bar{u}$ (m/s)	r_u (-)	$\bar{u}$ (m/s)	r_u (-)	$\bar{u}$ (m/s)	r_u (-)	$\bar{u}$ (m/s)	r_u (-)
10	1.32	0.12	0.92	0.11	0.90	0.12	0.98	0.11
11	1.28	0.12	0.94	0.11	0.95	0.12	1.01	0.11
12	1.25	0.12	0.96	0.11	0.99	0.13	1.04	0.12
13	1.22	0.13	0.98	0.11	1.03	0.13	1.07	0.12
14	1.18	0.13	1.00	0.12	1.08	0.14	1.10	0.12
15	1.14	0.14	1.02	0.12	1.12	0.15	1.12	0.12
16	1.11	0.15	1.05	0.12	1.16	0.16	1.15	0.12
17	1.07	0.16	1.07	0.13	1.20	0.16	1.18	0.12
18	1.04	0.17	1.09	0.13	1.24	0.17	1.21	0.12
19	1.11	0.17	1.04	0.13	1.15	0.17	1.15	0.13
20	0.96	0.18	1.13	0.13	1.33	0.18	1.26	0.13

Table 7.1: Mean velocity and turbulence intensity for a range of configurations and discharges. The values are extrapolated form the developed data base in chapter 5

Table 7.1 shows an example of the information that should be provided by the supplier. The values of table 7.1 are model results and they do not represent any scale prototype. However, the result show that the development of a table for larger configurations and discharge ranges is feasible in further studies. A table of values like the previous one will be a very handy designing tool in a design guideline

Depth parameter

The depth parameter (K_h), as previously mentioned, can be considered equal to 1 at the present study because the measurements were obtained close to the bottom. Moreover, Pilarczyk (2001) derived a value $K_h \approx 1$ for shallow and rough flow ($h/kr < 5$). In a different situation like a higher tailgate water depth, the supplier should decide between verifying the value for K_h or develop a table like table 7.1 that provides the flow parameter value close to the bottom.

Stability parameter

The stability parameter in the present equation is a key parameter on the design equation. Table 7.2 shows the derived values for the recorded failures. On the value, the stability parameter is no described as fix parameter, but as a mean value, a standard deviation and maximum and minimum values. If the design is based a deterministic approach, the maximum value should be used, by contrast, in a probabilistic approach, the mean and the standard deviation should be used.

$\bar{\Phi}$	σ_{Φ}	Max Φ	Min Φ
0,376	0,026	0,420	0,334

Table 7.2: The stability parameter, as the mean, the standard deviation, the maximum and the minimum values.

Safety factor

The design equation, as mentioned before, does not include any safety factor. Therefore, the decision of the applied safety factor relies on the judgment of the designer and the risk associated with failure of the block mattress. The failure of the block mattress is a sudden failure that cannot be predicted based on periodic inspections. However, the failure recorded at the studied situation did not lead to the complete removal of mattress, for larger discharges this failure is likely to occur.

Placement

Upstream edge

The placement of the upstream edge has a major importance on the design of the block mattress. The required thickness is calculated for a situation for a shielded front row. Thus, the placement should ensure that the front is not exposed to the flow from the apron. The exposed area of the front row will lead to failure for discharges smaller than the design one. Moreover, the failure of the first row implies a higher risk for the stability of the structure.

Downstream edge

At chapter four, a detailed explanation of the flow around the last row of blocks. The weakness of this point is based on the acceleration due to the behaviour as a backwards facing step and the lack of cohesion supplied by the adjacent blocks. Thus, particular care should be taken on the downstream edge. For example, a layer of lose stone placed downstream. Moreover, an alternative shape for the last block was proposed in chapter 4, which behaviour should be checked.

References

Bulmer, M. ed., (1979). 4. Descriptive properties of distributions. In: Principles of statistics, 1st ed. [online] Dover Publications. Available at: http://bobweigel.net/csi763/images/Bulmer_Principles_of_Statistics_1979_all.pdf [Accessed 5 Jun. 2017].

Brighthub Engineering. (2017). *Measuring Open Channel Flow Rates with a weir or a flume*. [online] Available at: http://www.brighthubengineering.com/hydraulics-civil-engineering/51435-introduction-to-the-weir-and-flume/ [Accessed 14 Feb. 2017].

CIRIA, CUR, CETMEF. (2007). *The Rock Manual. The use of rock in hydraulic engineering (2nd edition).* C683, CIRIA, London.

De Gunst, M. (1999). *Stone stability in a turbulent flow behind a step.* M.Sc. thesis, Delft University of Technology. (In dutch) In: (Hofland, 2005)

Emiroglu, M. and Ikinciogullari, E. (2016). Determination of discharge capacity of rectangular side weirs using Schmidt approach. *Flow Measurement and Instrumentation*, 50, pp.158-168. `

Einstein, H. and El-Samni, E. (1949). Hydrodynamics forces on a rough wall. *Reviews of Modern Physics*, 21(3): 520-524. In (Uitteenbogaard, R., Hoffmans, G. and Akkerman, G. 1999).

Escarameia M, and May R. W. P. (1992). Channel protection – turbulence downstream of structures. HR Report SR 313

Escarameia M. (1995). Channel protection – Gabion mattresses and Concrete blocks. HR Reports SR 427

García, C., Cantero, M., Niño, Y. and García, M. (2005). Turbulence Measurements with Acoustic Doppler Velocimeter. *Journal of Hydraulic Engineering*, 131(12), pp.1062-1073.

Gharahjeh, S., Aydin, I. and Altan-Sakarya, A. (2015). Weir velocity formulation for sharp-crested rectangular weirs. *Flow Measurement and Instrumentation*, 41, pp.50-56.

Goldbold, J. (2014). Stability design for concrete mattresses. In *Twenty-fourth (2014) International Ocean and Polar Engineering Conference*, pages 302-308, Busan, Korea. Int. Society of Offshore and Polar Engineers.

Grass, A. (1970). Initial stability of fine bed sands. *Journal of the Hydraulics Civision, Proceedings of* ASCE, 96(HYE):619-632

Heller, V. (2011). Scale effects in physical hydraulic engineering models. Journal of Hydraulic Research, 49(3), pp.293-306.

Hoan, N. T. (2008). Stone stability under non-uniform flow. *Ph.D. thesis*. Delft University of Techonology.

Hoan, N.T., Stive, M.J.F., Booij, R., Verhagen, H.J. (2011). Stone stability in non-uniform flow. *Journal Hydraulic Engineering*.

Hofland, B (2005). Rock and Roll: *turbulence-induced damage to granular bed protections.* Ph.D. thesis, Delft University of Technology

Hinze, J.O *Turbulence: an introduction to its mechanism and theory*. McGraw-Hill, New York, N.Y, 1959. In (Schiereck 2012)

Ibrahim, M. (2015). Bed profile downstream compound sharp crested V-notch weir. *Alexandria Engineering Journal*, 54(3), pp.607-613.

Ibrahim, M. (2016). Bed Configurations of Downstream Sharp Crested Weir with Orifices. *Journal of Scientific Research and Reports*, 9(2), pp.1-16.

Jongeling, T., Blom, A., Jagers, H.R.A. and

Stolker, C. (2003). Design method granular protections. Technical Report Q2933/Q3018, WL| Delft Hydraulics.

Kang, J., Jung, S., Rhee, D. and Yeo, H. (2011). Experimental Study for the Determination of the Material Diameter of the Riprap Bed Protection. *Engineering*, 03(10), pp.992-1001.

Kim, J., Moin, P. and Moser, R. (1987). Turbulence statistics in fully developed channel flow at low Reynolds number. Journal of Fluid Mechanics, 177(-1), p.133.

McPherson, G. (2015). *Shetland Tidal Array Cable Protection Risk Assessment*. Edinburg: Nova Innovation Ltd.

Nezu, I. and Nakagawa, H. (1993). *Turbulence in Open-Channel flows.* Balkema Rotterdam. In (Hofland 2005)

PIANC (2015) Guidelines for protecting berthing structures from scour caused by ships. Brussels: PIANC

Pilarczyk, K. (2000). *Geosynthetics and geosystems in hydraulic and coastal engineering*. 1st ed. Rotterdam: A.A. Balkema.

Pilarczyk, K. (2001) Unification of stability formulae for revertments. In Porg. XXIX IAHR *congress, Beijing*

Pilarczyk, K.W. (2003). *Design of revetments.* Rijkswaterstaat, DWW.

Qingfu, X. and Zhiping, L. (2012). Study on Flow Reattachment Length. *Procedia Engineering*, 28, pp.527-533.

Schiereck, G.J. updated by Verhagen, H.J. (2012). *Introduction to Bed, bank and shore protection.* VSSD.

Shields, A. (1936) *Anwendung der Aehnlichleitsmechanik und der Turbulenz-forschung auf die Geschiebebewegung.* Mitteilungen der Preussischen Versuchsanstalt fur Wasserbau und Schiffbau, Helft 26, Berlin. In German. In (Hoan, 2008)

Smyrnis, A. Stability of block mats under flow conditions M.Sc. thesis, Delft University of Technology.

Sobeih, M. (2012). Scour depth downstream weir with openings. *INTERNATIONAL JOURNAL OF CIVIL AND STRUCTURAL ENGINEERING*, 3(1), pp.259-270.

Steenstra, R.S. (2014). *Incorporation of the effects of accelerating flow in the design of granular bed protections.* M.S. Thesis, Delft University of Technology.

Song, T. and Chiew, Y. (2001). Turbulence Measurement in Nonuniform Open-Channel Flow Using Acoustic Doppler Velocimeter (ADV). *Journal of Engineering Mechanics*, 127(3), pp.219-232.

Thompson, C. (2017). *Coastal Sediment Dynamics*. University of Southampton. Lecture notes.

Uitteenbogaard, R., Hoffmans, G. and Akkerman, G. (1999). *Turbulence schematization for stone stability assessment*. Delft: Delft Hydraulics.

Uijttewaal, W. *Turbulence in Hydraulics*. Delft University of Technology. Lecture notes

Van Velzen, G., De Jong, M.P.C. (2015). *Propeller jets, Knowledge gap 15a - Stability of a block mattress in propeller-induced loads.* Deltares.

Voulgaris, G. and Trowbridge, J. (1998). Evaluation of the Acoustic Doppler Velocimeter (ADV) for Turbulence Measurements*. *Journal of Atmospheric and Oceanic Technology*, 15(1), pp.272-289.

Annex 1: Betomat block mattress

Betomat -Type GS-VB

- The Betomat is a registered trademark of Holcim Betoprodukten bv, Aslst, Nedelands.
- The present prototype block mattress documentation was obtained for Van Velzen and De Jong (2015)

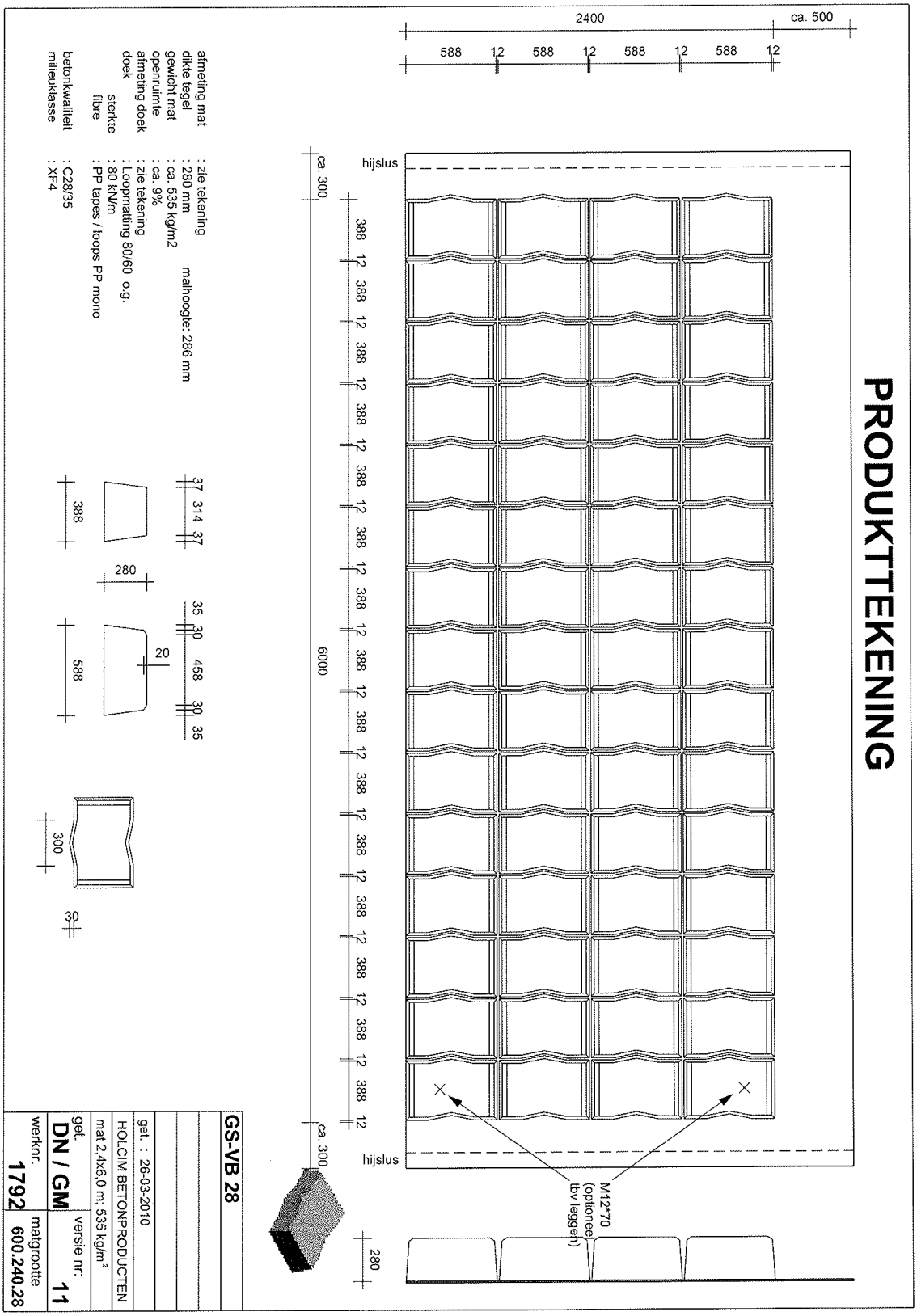
PRODUKTTEKENING
2400
ca. 500
588 12 588 12 588 12 588 12
hijslus
ca. 300
6000
388 12
hijslus
ca. 300
280
M12*70
(optioneel
tbv leggen)
afmeting mat : zie tekening
dikte tegel : 280 mm
gewicht mat : ca. 535 kg/m2
openruimte : ca. 9%
afmeting doek : zie tekening
doek : Loopmatting 80/60 o.g.
sterkte : 80 kN/m
fibre : PP tapes / loops PP mono
betonkwaliteit : C28/35
milieuklasse : XF4
malhoogte: 286 mm
37 314 37
388
280
35 30 458 30 35
20
588
300
30
GS-VB 28
get. : 26-03-2010
HOLCIM BETONPRODUCTEN
mat 2,4x6,0 m; 535 kg/m²
get.
DN / GM
versie nr.:
11
werknr.
1792
matgrootte
600.240.28

Annex 2: Model block mattress

- The model block mattress is based of the Betomat GS-VB
- The Betomat is a registered trademark of Holcim Betoprodukten bv, Aslst, Nedelands.
- The present model block mattress documentation was obtained for Van Velzen and De Jong (2015)

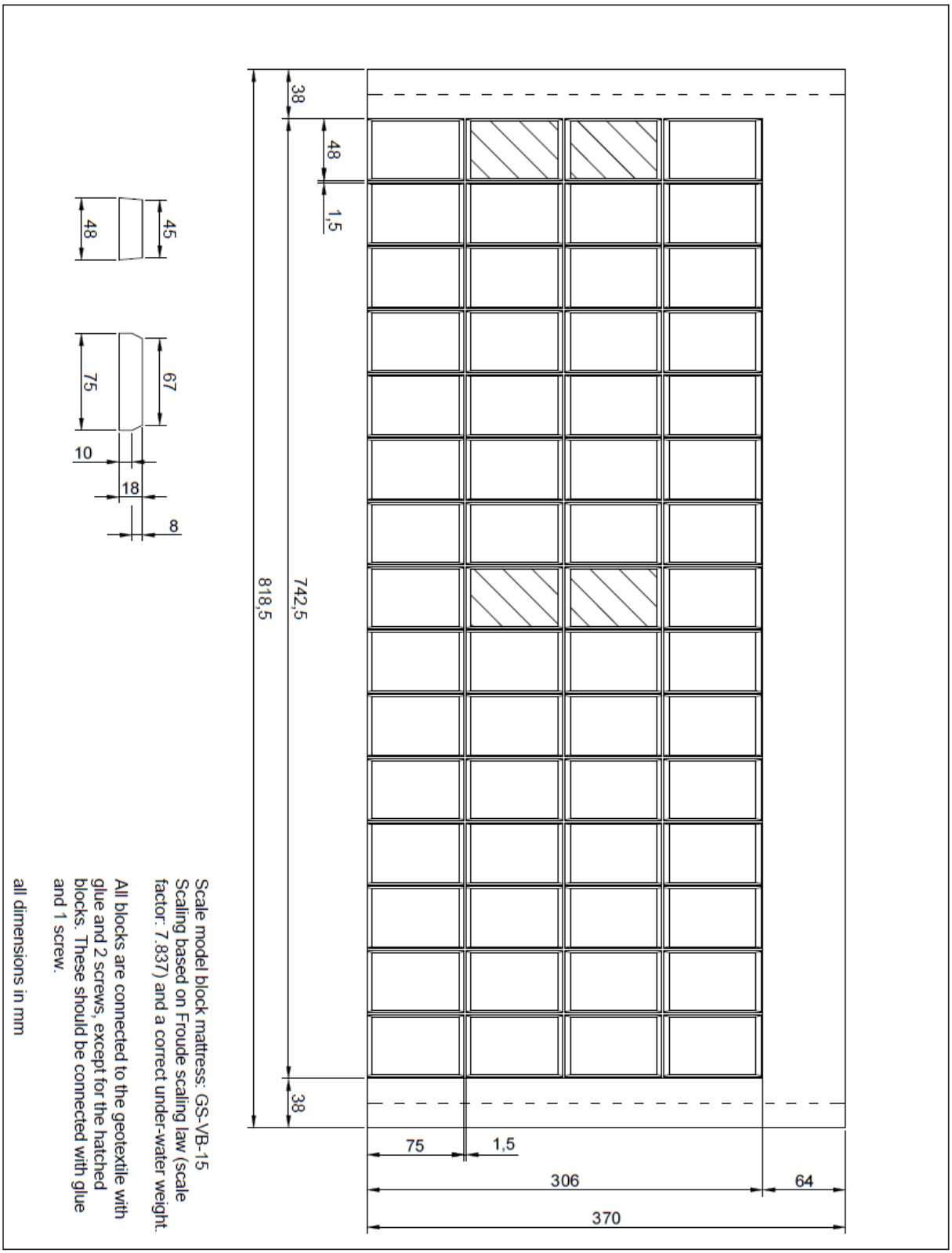

Scale model block mattress: GS-VB-15
Scaling based on Froude scaling law (scale factor: 7.837) and a correct under-water weight.

All blocks are connected to the geotextile with glue and 2 screws, except for the hatched blocks. These should be connected with glue and 1 screw.

all dimensions in mm

Annex 3: Discharge calculation

Te calculation of the discharge is based on two different devices, the measurement at the pipeline and the measurement at an accuratelly calibrated weir height and rehbock equation. At the weir measurement the discharge needs around 15 minutes to stabilize, thus, a values tranformation was done. In this process both water height and the displayed discharge at the pipeline were measured and compared. Equation 1 shows the rehbock equation to derived the discharge based on the water height at the weir. Besides, table 1 shows the derived values table.

$$Q = 1000 \cdot ce \cdot \frac{2}{3}\sqrt{2g} \cdot b \cdot h_e^{1.5} \qquad [l/s] \qquad [1]$$

Where:

$$h_e = h_a + 0.0012 \quad [m] \qquad [2]$$

$$c_e = 0.602 + 0.083 \frac{h_a}{h_b} \quad [-] \qquad [3]$$

$$g = 9.81 \quad [m/s^2] \qquad [4]$$

$$b = 0.442 \quad [m] \qquad [5]$$

$$h_b = 0.25 \quad [m] \qquad [6]$$

$$h_b = Water\ level\ at\ the\ weir \quad [m] \qquad [7]$$

Pipe discharge [l/s]	Water Depth [cm]	Real Discharge [l/s]	Error [%]
3,9	30,8	4,57	14,66
6,8	43,8	7,68	11,46
10,7	58,3	11,77	9,09
14	69,9	15,47	9,50
16,9	78,8	18,55	8,89
17,7	81,1	19,38	8,67
18,9	84,9	20,78	9,05
21,9	93	23,88	8,29
22,7	95,1	24,71	8,13
24,1	98,8	26,2	8,02
26,8	106,1	29,23	8,31
28,3	109,6	30,37	6,82
31,2	117	33,99	8,21
33,1	121,3	35,94	7,90
34,3	124	37,19	7,77
36,5	129,1	39,588	7,80
37,9	132,3	41,12	7,83

Table A3.1: Values for the pipe and real discharge and the relative errors

Annex 4: Turbulence intensity measurements

σ_u [m/s]	σ_w [m/s]	σ_u/σ_w [-]	σ_u [m/s]	σ_w [m/s]	σ_u/σ_w [-]
0,149	0,086	1,729	0,159	0,081	1,979
0,147	0,089	1,645	0,134	0,082	1,638
0,148	0,091	1,626	0,159	0,084	1,899
0,150	0,094	1,597	0,156	0,084	1,850
0,148	0,091	1,633	0,162	0,088	1,849
0,148	0,089	1,659	0,164	0,090	1,825
0,147	0,090	1,630	0,160	0,088	1,824
0,148	0,090	1,646	0,164	0,086	1,892
0,150	0,092	1,620	0,167	0,088	1,905
0,150	0,091	1,652	0,160	0,088	1,832
0,153	0,077	1,980	0,155	0,086	1,810
0,149	0,078	1,908	0,104	0,063	1,665
0,163	0,081	2,028	0,114	0,066	1,725
0,156	0,079	1,965	0,130	0,080	1,635
0,152	0,080	1,910	0,122	0,071	1,710
0,162	0,081	2,004	0,126	0,078	1,615
0,159	0,085	1,877	0,131	0,074	1,763
0,158	0,081	1,946	0,144	0,082	1,760
0,156	0,082	1,904	0,142	0,081	1,749
0,171	0,086	1,979	0,149	0,088	1,708
0,179	0,088	2,033	0,147	0,084	1,747
0,178	0,090	1,986	0,154	0,086	1,797
0,180	0,087	2,082	0,155	0,086	1,810
0,179	0,086	2,082	0,163	0,092	1,764
0,160	0,086	1,855	0,156	0,088	1,774
0,178	0,091	1,952	0,163	0,099	1,642
0,183	0,091	2,006	0,149	0,093	1,599
0,179	0,090	1,982	0,155	0,091	1,707
0,134	0,074	1,801	0,155	0,093	1,667
0,144	0,083	1,726	0,135	0,081	1,679
0,148	0,085	1,746	0,153	0,080	1,908

Table A4.1: Turbulence intensity in streamwise and vertical direction and the ratio between them

Annex 5: Failure signals

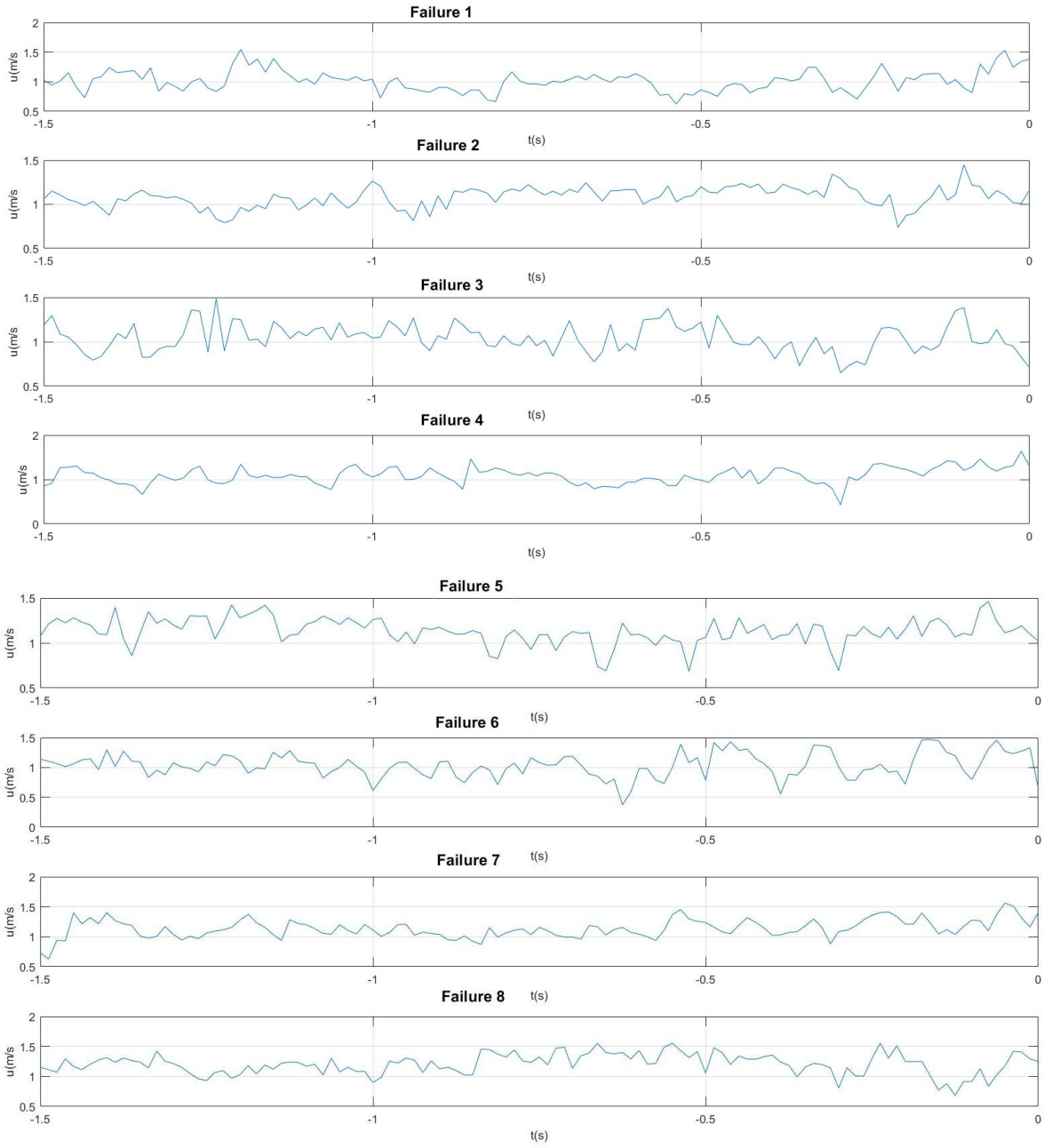

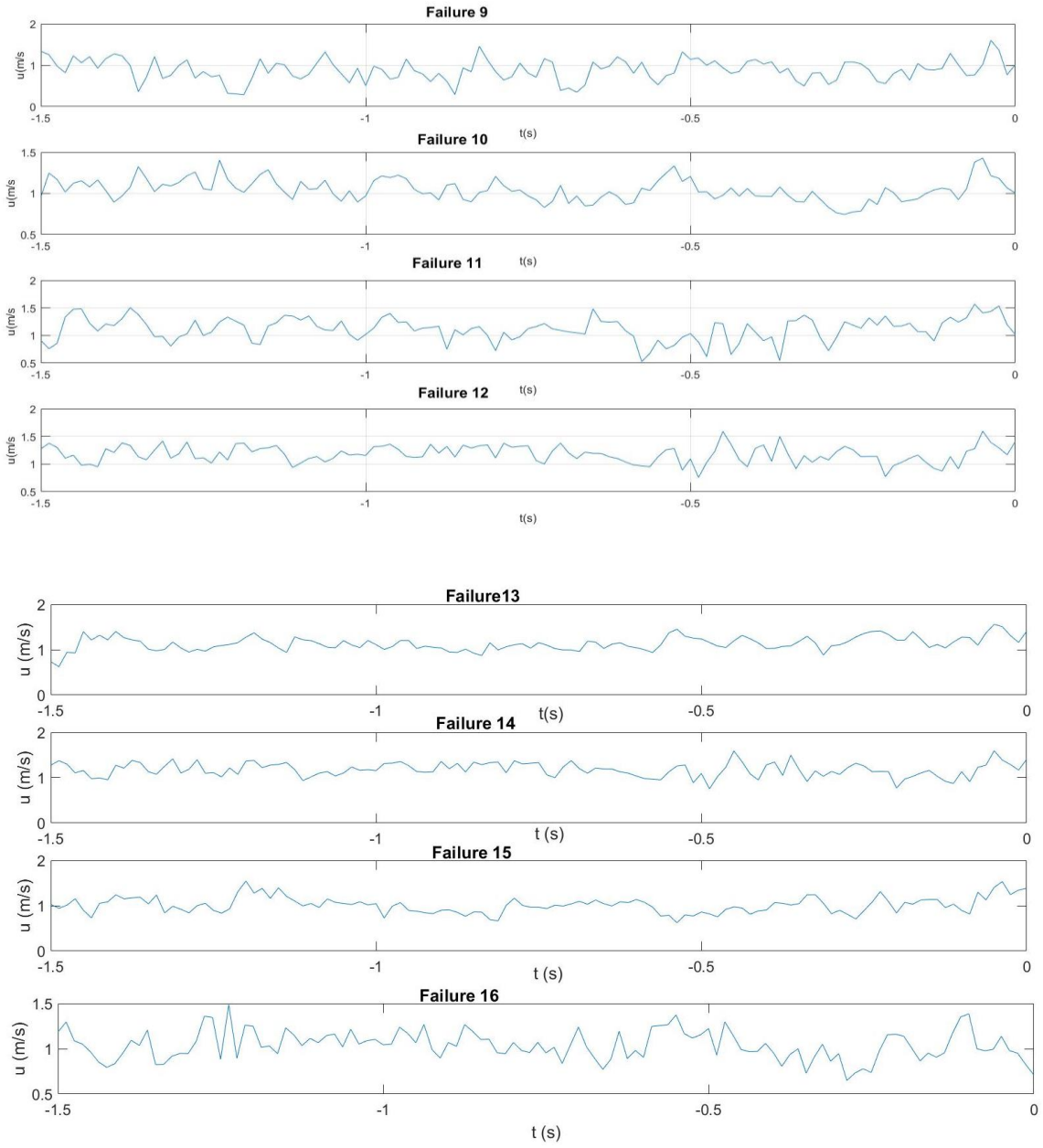

Figure A5.1: Signals of the recorded 16 failures. The failure moment is located a t = 0

List of figures

List if tables

List of symbols

Roman symbols

A	Area	m^2
C	Turbulent coefficient (Escarameia)	[-]
C_D	Drag coefficient	[-]
C_F	Friction coefficient	[-]
C_L	Lift coefficient	[-]
D	Characteristic dimension (Pilarczyk)	[m]
d	Stone diameter	[m]
D_{n50}	Median nominal diameter	[m]
F_D	Drag force	[N]
F_F	Friction force	[N]
F_G	Gravity force	[N]
F_L	Lifting force	[N]
g	Gravitational acceleration	m/s^2
h	Water depth	[m]
hm	Jongeling characteristic length	[m]
k	Turbulence kinetic energy	m^2/s^2
K_h	Water depth parameter (Pilarczyk)	[-]
K_T	Turbulence parameter (Pilarczyk)	[-]
Qi	Raupach quadrant	[-]
r_i	Relative turbulence intensity	[-]
Re	Reynolds number	[-]
TI	Turbulence intensity (Escarameia)	[%]
u	Streamwise velocity	[m/s]
u_*	Friction velocity	[m/s]
u_b	Streamwise near-bed velocity	[m/s]
U_{ave}	Streamwise velocity averaged over the vertical	[m/s]
U_{fail}	Failure streamwise velocity	[m/s]
U_{peak}	Peak of streamwise velocity associated to failure	[m/s]
v	Transverse velocity	[m/s]
V	Volume	$[m^3]$
w	Vertical velocity	[m/s]
x	Streamwise coordinate	m
y	Transverse coordinate	m

z	Vertical coordinate	m

Greek symbols

α	Empirical constant (Various uses)	[-]
α_{peak}	Turbulence magnification factor derived based on peak velocities	[-]
α_{op}	Turbulence magnification factor derived based on failure velocity optimization	[-]
β	Empirical constant (Various uses)	[-]
Δ	Specific submerged density	[-]
δ	Error	[-]
κ	Von-Kartman constant	[-]
ρ	Water density	[Kg/m^3]
ρ_s	Solid density	[Kg/m^3]
φ	Stability parameter (Pilarczyk)	[-]
τ_{xz}	Shear stress	[N/m^2]
Ψ	Shield parameter	[-]
Ψ_{Lm}	Stability parameter (Jongeling)	[-]
Ψ_{WL}	Stability parameter (Hofland)	[-]
$\Psi_{u-\sigma[u]}$	Stability parameter (Hoan)	[-]

Mathematical symbols

σ_x	Standard deviation
$\bar{x}$	Average over time
$\overline{x'^2}$	Square root average
x'	Fluctuating part of x around $\bar{x}$
$\lvert x \rvert$	Absolute value
$\langle x \rangle_L$	Spatial average of x over L
$\overline{u'w'}$	Reynold stress

Abbreviations

2D	Two-dimensional
3D	Three-dimensional
ADV	Acoustic Doppler velocimeter
BFS	Backwards facing step

EMS	Electromagnetic Magnetic velocimeter Sensor
QSF	Quasy-steady forces
LDV	Laser Doppler velocimeter
TWP	Turbulence wall pressures

Acknowledgments

This thesis would be impossible to develop without the support of many people. First, I would like to thank to Holcim Coastal B.V. for making the study possible. Thank you to all my committee members and all the staff of the water lab for all the support given.

Besides, I will like to thank to all my lectures from all the universities I have been during my master for all the knowledge provided. I would also like to thank to all the people that make CoMEM possible and giving to me this amazing experience.

Thank you to my colleges from CoMEM for this two years of fun, struggling and Friday beers and kapsalons. Thank you to my family of RC Delft for making be felling home during these two seasons. Thank to my family and friends for all the support given during this two years and specially to my old friend Bombin because you will always be present in all the achievements of my live.

Finally, thank you to my travel partner for sharing once again this stage of our adventure.